LETTERS
https://doi.org/10.1038/s41591-020-01194-5

nature medicine

Check for updates

T cell and antibody responses induced by a single dose of ChAdOx1 nCoV-19 (AZD1222) vaccine in a phase 1/2 clinical trial

Katie J. Ewer[1,18]✉, Jordan R. Barrett[1,18], Sandra Belij-Rammerstorfer[1,18], Hannah Sharpe[1], Rebecca Makinson[1], Richard Morter[1], Amy Flaxman[1], Daniel Wright[1], Duncan Bellamy[1], Mustapha Bittaye[1], Christina Dold[2], Nicholas M. Provine[3], Jeremy Aboagye[1], Jamie Fowler[1], Sarah E. Silk[1], Jennifer Alderson[4], Parvinder K. Aley[2], Brian Angus[3], Eleanor Berrie[5], Sagida Bibi[2], Paola Cicconi[2], Elizabeth A. Clutterbuck[2], Irina Chelysheva[2], Pedro M. Folegatti[1], Michelle Fuskova[1], Catherine M. Green[5], Daniel Jenkin[1], Simon Kerridge[2], Alison Lawrie[1], Angela M. Minassian[1], Maria Moore[2], Yama Mujadidi[2], Emma Plested[2], Ian Poulton[1], Maheshi N. Ramasamy[2], Hannah Robinson[2], Rinn Song[2], Matthew D. Snape[2], Richard Tarrant[5], Merryn Voysey[2], Marion E. E. Watson[1], Alexander D. Douglas[1], Adrian V. S. Hill[1,18], Sarah C. Gilbert[1,18], Andrew J. Pollard[2,18], Teresa Lambe[1,18]✉ and the Oxford COVID Vaccine Trial Group*

Severe acute respiratory syndrome coronavirus 2 (SARS-CoV-2), the causative agent of Coronavirus Disease 2019 (COVID-19), has caused a global pandemic, and safe, effective vaccines are urgently needed[1]. Strong, Th1-skewed T cell responses can drive protective humoral and cell-mediated immune responses[2] and might reduce the potential for disease enhancement[3]. Cytotoxic T cells clear virus-infected host cells and contribute to control of infection[4]. Studies of patients infected with SARS-CoV-2 have suggested a protective role for both humoral and cell-mediated immune responses in recovery from COVID-19 (refs. [5,6]). ChAdOx1 nCoV-19 (AZD1222) is a candidate SARS-CoV-2 vaccine comprising a replication-deficient simian adenovirus expressing full-length SARS-CoV-2 spike protein. We recently reported preliminary safety and immunogenicity data from a phase 1/2 trial of the ChAdOx1 nCoV-19 vaccine (NCT04400838)[7] given as either a one- or two-dose regimen. The vaccine was tolerated, with induction of neutralizing antibodies and antigen-specific T cells against the SARS-CoV-2 spike protein. Here we describe, in detail, exploratory analyses of the immune responses in adults, aged 18–55 years, up to 8 weeks after vaccination with a single dose of ChAdOx1 nCoV-19 in this trial, demonstrating an induction of a Th1-biased response characterized by interferon-γ and tumor necrosis factor-α cytokine secretion by CD4$^+$ T cells and antibody production predominantly of IgG1 and IgG3 subclasses. CD8$^+$ T cells, of monofunctional, polyfunctional and cytotoxic phenotypes, were also induced. Taken together, these results suggest a favorable immune profile induced by ChAdOx1 nCoV-19 vaccine, supporting the progression of this vaccine candidate to ongoing phase 2/3 trials to assess vaccine efficacy.

Efforts to develop a vaccine against SARS-CoV-2 to control the global COVID-19 disease pandemic have been underway since January 2020, with more than 40 vaccine candidates in clinical trials by October 2020[1]. The past decade has seen an expansion and acceleration in the development of tools to support pandemic preparedness, including the development of vaccines against novel and emerging pathogens[8,9]. This acceleration, spurred on by numerous outbreaks of diseases, including SARS-CoV, MERS-CoV, Ebola and Zika, has leveraged the use of platform technologies and blueprints for target product profiles for priority diseases[10]. Replication-deficient adenoviruses[11] are attractive for use as COVID-19 vaccine candidates, as they can be manufactured at scale, have favorable safety profiles and are highly immunogenic. Importantly, viral vectored vaccines can induce strong immune responses in older adults and immunocompromised individuals[12,13]. Replication-deficient adenovirus vectors are also potent inducers of both antibodies as well as cytotoxic T cells; the latter can clear virus-infected host cells and contribute to the control of infection, alleviating disease symptoms[4,14]. Importantly, high-frequency T cell responses targeting the SARS-CoV-2 spike protein have been detected in patients who recover from COVID-19, with recent data suggesting a role for T cells during COVID-19 (refs. [15–17]).

Previous efforts to develop vaccines against human coronaviruses have faced challenges, with several preclinical studies demonstrating disease enhancement in vaccinated animals after viral

[1]The Jenner Institute, University of Oxford, Oxford, UK. [2]Oxford Vaccine Group, Department of Paediatrics, University of Oxford, Oxford, UK. [3]Nuffield Department of Medicine, University of Oxford, Oxford, UK. [4]The Kennedy Institute of Rheumatology, University of Oxford, Oxford, UK. [5]Clinical Biomanufacturing Facility, Nuffield Department of Medicine, University of Oxford, Oxford, UK. [18]These authors contributed equally: Katie J. Ewer, Jordan R. Barrett, Sandra Belij-Rammerstorfer, Adrian V. S. Hill, Sarah C. Gilbert, Andrew J Pollard, Teresa Lambe. *A list of authors and their affiliations appears at the end of the paper. ✉e-mail: katie.ewer@ndm.ox.ac.uk; Teresa.lambe@ndm.ox.ac.uk

challenge. This was characterized by eosinophilic infiltrates resulting in immunopathology, after the induction of a T helper cell type 2 (Th2)-biased response, or a weak neutralizing antibody response that might contribute to antibody-dependent enhancement of infection[3]. In-depth analysis of SARS-CoV-2 vaccines are being conducted to determine whether responses are Th1 or Th2 dominated; these types of studies are being implemented in several COVID-19 vaccine trials[18–21].

ChAdOx1 nCoV-19 (AZD1222) is a replication-deficient simian adenoviral vector that expresses the full-length SARS-CoV-2 spike protein. In preclinical studies, either a single dose or two doses of ChAdOx1 nCoV-19 vaccination prevented SARS-CoV-2-mediated pneumonia in rhesus macaques[22]. We previously reported safety data from phase 1/2 studies and demonstrated induction of SARS-CoV-2 spike-specific antibodies after vaccination, with boosting of binding and neutralizing titers after a second dose[7]. These data supported progression to phase 3 trials with a two-dose regimen, and we have now expanded our immunogenicity analysis to explore a wider range of the immunological phenotypes induced. In an accompanying paper[23], we present detailed functional antibody profiling of responses to prime-boost regimens with differing doses and intervals.

Currently, there are no defined correlates of protection against COVID-19 infection, and the immunological thresholds required for vaccine efficacy remain undefined[24]. Clinical studies have suggested a protective role for both humoral and cell-mediated immunity in recovery from SARS-CoV-2 infection[5,6,25]. Here we provide a detailed description of the immune response after administration of one dose of ChAdOx1 nCoV-19. We define, in detail, the isotypes, subclasses and antibody avidity induced after vaccination and also perform multiplex cytokine profiling and intracellular cytokine staining (ICS) analysis, demonstrating that ChAdOx1 nCoV-19 vaccination induces a predominantly Th1-type response.

Results

Study participants. Recruitment, vaccination and demographics of the study participants were previously reported, with interim safety and immunogenicity data[7]. Healthy adults aged 18–55 years ($n=88$) were randomized to receive either 5×10^{10} viral particles of ChAdOx1 nCov-19 or control vaccine (MenACWY) (Group 1; Supplementary Fig. 1). Blood samples were collected on the day of vaccination and 7, 14, 28 and 56 d after vaccination. Supplementary Table 1 summarizes the number of individuals assessed in each assay.

Immune cell activation induced by ChAdOx1 nCoV-19 vaccination with Th1-biased cytokine secretion. An unbiased approach was applied to measure gross phenotypic and cellular changes on days 7, 14 and 28 after vaccination (Fig. 1a–e). Flow cytometric and combined t-distributed stochastic neighbor embedding (tSNE) analysis of 26 randomly selected ChAdOx1 nCoV-19 vaccinated volunteers showed discrete populations of T cells, natural killer (NK) cells and B cells. Within these clusters, distinct populations of proliferating (Ki-67$^+$) or activated (CD69$^+$) cells were identified (Fig. 1b–e). B cells, especially the IgG$^+$ B cell population, upregulated Ki-67 at all post-vaccination time points (Fig. 1f,g). Within the total B cell population, the shift toward an activated phenotype peaked on days 7–28 and for the IgG$^+$ B cell population on days 7–14 (Fig. 1f,g).

CD4$^+$ T cells had increased expression of CD69 on days 7–28 after vaccination and a trend toward increased Ki-67 expression at days 7 and 14 after vaccination (Fig. 1f,g)[26]. CD8$^+$ T cells expressed a similar pattern of Ki-67 and CD69 expression between days 7 and 28 after vaccination (Fig. 1f,g). We did not detect increases in expression of terminal differentiation markers CD57 and KLRG1 in post-vaccination CD8$^+$ T cells (Supplementary Fig. 2), which would indicate a reduction in post-vaccination cytotoxic capacity[27]. After peptide stimulation, an increase in tumor necrosis factor (TNF)-α and interferon (IFN)-γ production by CD4$^+$ T cells was also observed at day 14 (Fig. 1h).

NK cells can elicit a cytotoxic response to viral infection or vaccination[28,29]. Total expression of Ki-67 by NK cells increased steadily to a peak at day 28 (Fig. 1f). There was no significant change in the expression of CD57 or the activating receptor NKG2C (Supplementary Fig. 2).

Multiplex cytokine analysis was performed on day 7 after vaccination after antigen-specific stimulation of peripheral blood mononuclear cells (PBMCs) with pooled SARS-CoV-2 spike peptides. Of the nine cytokines analyzed, five (IL-1β, IL-12p70, IL-4, IL-13 and IL-8) showed no difference in expression levels after stimulation. IFN-γ and IL-2 levels after PBMC stimulation were significantly increased in individuals who received the ChAdOx1 nCoV-19 vaccine compared to MenACWY controls (***$P=0.0009$ and **$P=0.0027$, respectively, two-tailed Mann–Whitney test). IL-4 and IL-13 levels after PBMC stimulation were not elevated in individuals who received the ChAdOx1 nCoV-19 vaccine after stimulation of PBMCs ($P>0.05$ for both, two-tailed Mann–Whitney test), but a modest increase in IL-10 was measured (*$P=0.045$, two-tailed Mann–Whitney test). The magnitude of cytokine secretion measured in PBMC supernatant in individuals who received the ChAdOx1 nCoV-19 vaccine was greater for IFN-γ (median 36.4 pg ml^{-1}, interquartile range (IQR) 15–67) and IL-2 (median 10.7 pg ml^{-1}, IQR 1.7–22) than for IL-10 (median 1.4 pg ml^{-1}, IQR 0.9–2.6), indicating a strong potential bias toward secretion of Th1 cytokines in blood in response to stimulation with SARS-CoV-2 spike peptides (Fig. 1i).

Humoral and cellular immune responses to ChAdOx1 nCoV-19 do not differ by sex. Robust immunity induced by ChAdOx1

Fig. 1 | Activation of lymphocyte populations after ChAdOx1 nCoV-19 vaccination. a–e, tSNE analysis of 9,600,000 live lymphocytes from 26 ChAdOx1 nCoV-19 vaccine trial participants across four time points (D0 $n=24$, D7 $n=23$, D14 $n=25$ and D28 $n=24$). Two samples were not available, and six samples with fewer than 100,000 live lymphocytes were excluded. The tSNE plot was generated by concatenation of samples containing 100,000 randomly selected live lymphocytes from each sample. **a**, Global clustering of immune cells across all samples. **b–e**, tSNE population analysis at day 0 and days 7, 14 and 28 after vaccination. Areas of Ki-67$^+$ activity (yellow) cluster in IgG$^+$ B cells (1), NK cells (2) and CD4$^+$ T cells (3) after vaccination. Analysis conducted on unstimulated cells. **f–h**, Heat map analysis of activation markers expressed by immune cells at days 0, 7, 14 and 28 after ChAdOx1 nCoV-19 vaccination (D0 $n=24$, D7 $n=23$, D14 $n=25$ and D28 $n=24$). **f**, Expression of Ki-67 by IgG$^+$ B cells and NK cells (top two rows) and NK cells (top three rows). Expression of CD69 by CD4$^+$ T cells and CD8$^+$ T cells (bottom two rows). **g**, Expression of Ki-67 by B cells, CD4$^+$ T cells and CD8$^+$ T cells. **h**, Expression of TNF-α and IFN-γ by CD4$^+$ T cells. Analysis of TNF-α and IFN-γ expression conducted on cells stimulated with spike glycoprotein peptide pools with unstimulated values subtracted. All other analysis was conducted on unstimulated cells. **i**, A multiplex cytokine analysis was performed on day 7 after vaccination using supernatants after antigen-specific stimulation of PBMCs from ChAdOx1 nCov-19 (red) and MenACWY (blue). Number of samples presented: MenACWY–ChAdOx1 nCov-19: IFN-γ ($n=40,40$); IL-2 ($n=42,42$); TNF-α ($n=40,41$); IL-1β ($n=41,42$); IL-12p70 ($n=38,28$); IL-4 ($n=38,38$); IL-10 ($n=41,39$); IL-13 ($n=31,36$); and IL-8 ($n=42,41$). Individual data points are shown here as an aligned dot plot with lines showing the median with IQR. Significant differences were determined by two-tailed Mann–Whitney test with Bonferroni correction for multiple comparisons (***$P<0.001$; **$P<0.01$; *$P<0.05$).

nCOV-19 against the SARS-CoV-2 spike antigen, measured by ex vivo IFN-γ ELISpot and total IgG ELISA, was previously reported[7]. We analyzed these two main immunological outcome measures by sex and age (Supplementary Fig. 3). We found no sex difference in vaccine response at any of the time points measured (Supplementary Fig. 3a,b; $P > 0.05$, two-tailed Mann–Whitney test). We detected no association between age and magnitude of immune response for either outcome measure (Supplementary Fig. 3c) in this population aged between 18 and 55 years.

ChAdOx1 nCoV-19 vaccination induces SARS-CoV-2-specific IgM and IgA levels. Anti-SARS-CoV-2 IgG responses were detectable at day 14, peaked at day 28 and were maintained at day 56, as reported previously[7]. Here we show that vaccination with

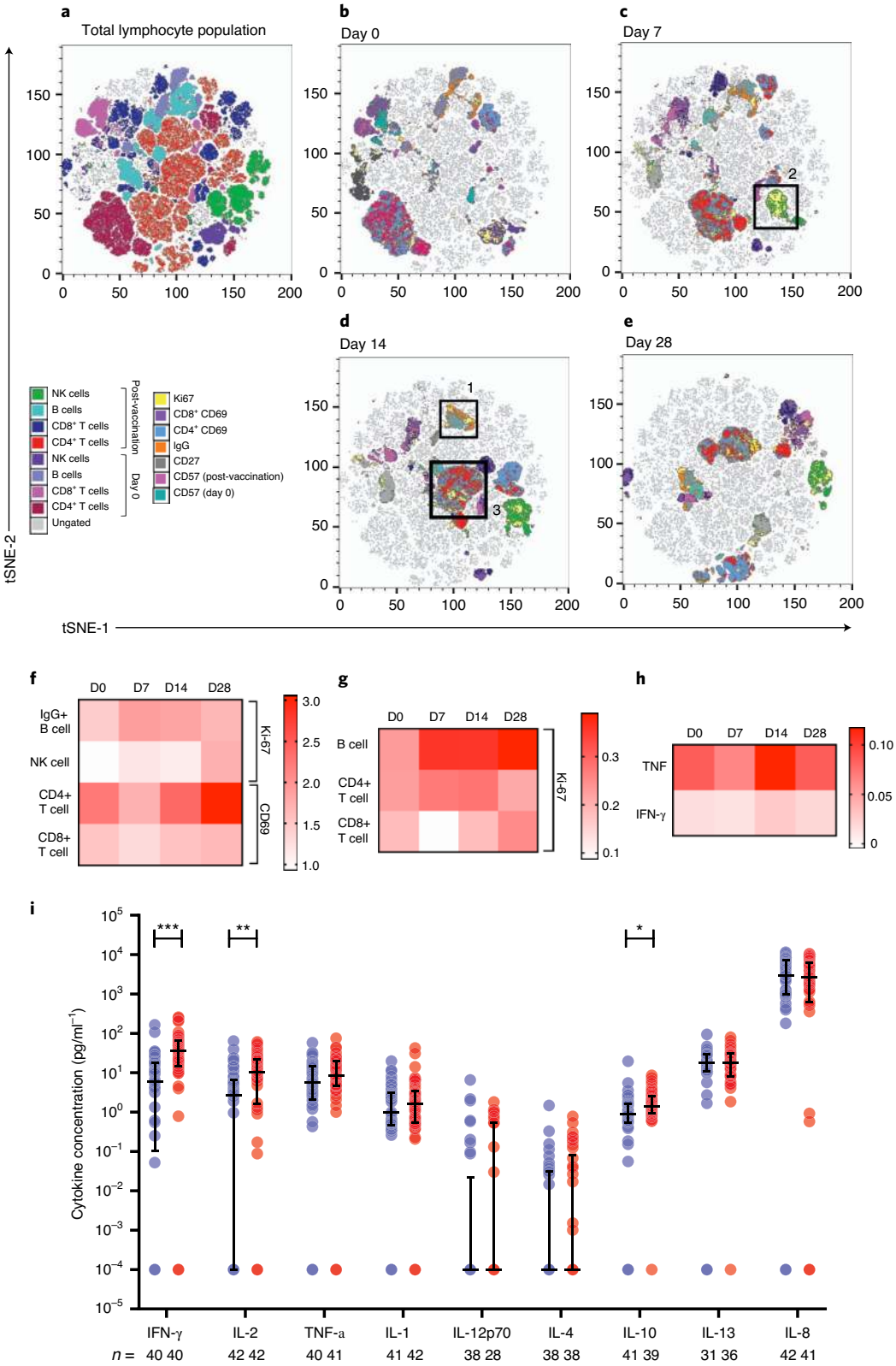

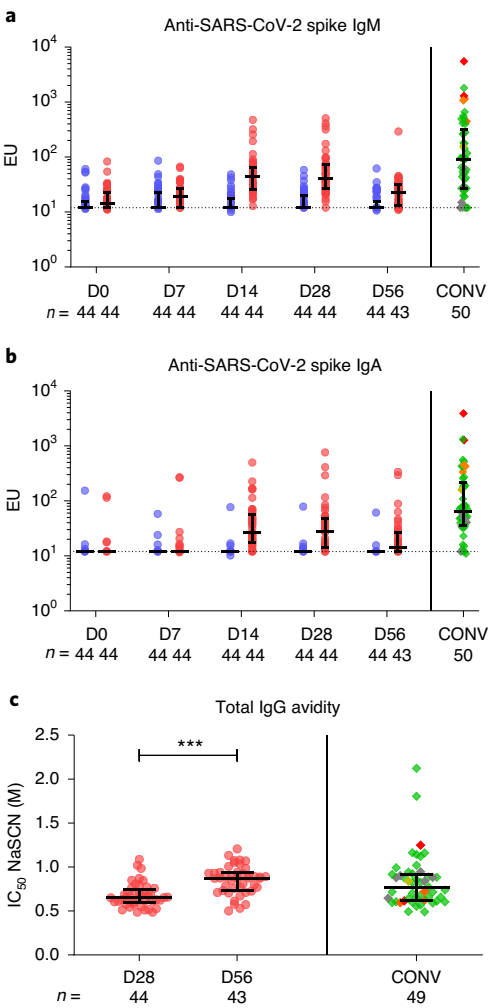

Fig. 2 | Immunoglobulin isotype responses induced by ChAdOx1 nCoV-19 vaccination. Volunteers received ChAdOx1 nCoV-19 (red) or MenACWY (blue) vaccination at day 0. SARS-CoV-2 spike trimer-specific IgM (**a**) and IgA (**b**) responses were quantified by standardized ELISA. Individual data points were expressed as ELISA units (EU) and shown here as an aligned dot plot with lines showing the median with IQR. Assays were performed at D0, D7, D14, D28 and D56 after vaccination ($n=44$ for all time points in both groups of volunteers, except for D56 in ChADOx1 nCoV19 where samples from only 43 volunteers were available). Dotted lines are shown at the limit of quantification of each assay. **c**, Avidity of SARS-CoV-2 spike trimer-specific IgG responses was measured using a NaSCN chemical displacement ELISA. Individual data points were expressed as an IC_{50} and shown here as scatter dot plots with lines showing the median with IQR. Assay was performed at D28 ($n=44$) and D56 after vaccination with ChAdOx1 nCoV-19 ($n=43$). Significant difference was determined by two-tailed Wilcoxon test (***$P<0.001$). CONV, convalescent plasma samples from patients with SARS-CoV-2 who recovered are shown here as a scatter dot plot with the line showing median with IQR (SARS-CoV-2 spike trimer-specific IgM, IgA $n=50$; IgG avidity $n=49$). CONV symbols are colored by disease severity: green, asymptomatic; gray, mildly symptomatic; yellow, moderately symptomatic; orange, severely symptomatic; and red, critically symptomatic.

ChAdOx1 nCoV-19 also generated increased levels of SARS-CoV-2 spike-specific IgM and IgA, with peak responses at day 14 or day 28, respectively (Fig. 2a,b and Supplementary Table 2). Low SARS-CoV-2 spike-specific IgE was detected after vaccination with ChAdOx1 nCoV-19, similar to that in convalescent patients with SARS-CoV-2 (Supplementary Fig. 4).

Anti-SARS-CoV-2 spike-specific IgG avidity increased significantly between day 28 (median 0.66, IQR 0.60–0.76; $n=44$) and day 56 (median 0.88, IQR 0.74–0.94; $n=44$) after vaccination (***$P<0.001$, two-tailed Wilcoxon test) (Fig. 2c). At day 56, IgG avidity induced by ChAdOx1 nCoV-19 vaccination was similar to that measured in plasma from convalescent patients with SARS-CoV-2 (median 0.77, IQR 0.62–0.92; $n=49$).

Subclass analysis after vaccination with ChAdOx1 nCoV-19. Specific IgG1 and IgG3 responses were readily detectable at day 14, increased by day 28 and returned to a similar level to that measured on day 14 by day 56 (Fig. 3a,b and Supplementary Table 2). Although IgG3 responses were quantifiable in nearly all individuals who received the vaccine (day 14, 39/44; day 28, 42/44; and day 56, 39/44), IgG1 responses were quantifiable in approximately half (day 14, 24/44; day 28, 23/44; and day 56, 22/44). Median levels of IgG2 and IgG4 were low across all time points (Fig. 3c,d). A similar IgG3/IgG1 profile with low levels of IgG2 and IgG4 was measured in convalescent plasma samples. In agreement with previously reported data[30], SARS-CoV-2 spike-specific IgG1 was below the limit of quantitation in some convalescent plasma samples (Fig. 3a).

ChAdOx1 nCoV-19 induces a broad T cell response to the S1 and S2 subunits of the SARS-CoV-2 spike antigen. Vaccine-specific T cell responses were measured by IFN-γ ELISpot before and after vaccination with ChAdOx1 nCoV-19, peaking at day 14 (ref. [7]), and summed T cell responses to the peptide pools for this cohort have been previously reported[7]. Responses were assayed against 13 pools of overlapping peptides (Supplementary Table 3) spanning the length of the vaccine antigen insert, which includes the S1 and S2 subunits, and an exogenous human tissue plasminogen activator (tPA) leader signal sequence peptide previously shown to enhance immunogenicity of a MERS-CoV vaccine candidate in mice[31]. There was a significant increase in response against both subunits between D0 and D14 (Fig. 4a; $n=42$ participants, $P<0.0001$ for both S1 and S2 comparing D0 to D14, two-tailed Wilcoxon matched pairs test). All pools except tPA elicited a positive response in at least 24% of participants (defined as the median of the negative control plus four standard deviations), indicating recognition of multiple epitopes across the spike antigen (Fig. 4b; $n=42$). The most frequently recognized pools were 4 and 2, which span amino acids 311–430 and 101–200 of the S1 domain and generated a positive response by IFN-γ ELISpot in 35/42 (83%) and 33/42 (78%) participants, respectively. Responses at D14 were also plotted as fold change from D0 (Fig. 4b and Supplementary Fig. 5), and the greatest increases were to pools 4 and 5. These pools elicited a median response of 146 spot-forming cells (SFCs)/10^6 PBMCs and 80 SFCs/10^6 PBMCs, respectively, at day 14, equating to a median of a 27- and 18-fold change from baseline.

Vaccination induces a Th1-biased CD4$^+$ and CD8$^+$ T cell response against SARS-CoV-2 spike peptides. Flow cytometry with ICS of PBMCs stimulated with peptides spanning the S1 and S2 subunits of SARS-CoV-2 spike protein demonstrated antigen-specific cytokine secretion from both CD4$^+$ (median 0.12, IQR 0.061–0.16) and CD8$^+$ (median 0.074, IQR 0.036–0.12) T cells 14 d after a single dose of ChAdOx1 nCoV-19 (Fig. 4c). CD8$^+$ T cells expressing the degranulation marker CD107a, indicating cytotoxic function, were detected after vaccination (median 0.038, IQR 0.012–0.066; Fig. 4d). CD4$^+$ responses were heavily biased toward secretion of Th1 cytokines (IFN-γ and IL-2) rather than Th2 (IL-5 and IL-13; Fig. 4e) The frequency of cytokine-positive cells was generally higher in the CD4$^+$ T cell population than the CD8$^+$ T cell population, and cytokine responses were detected at day 14 from participants with

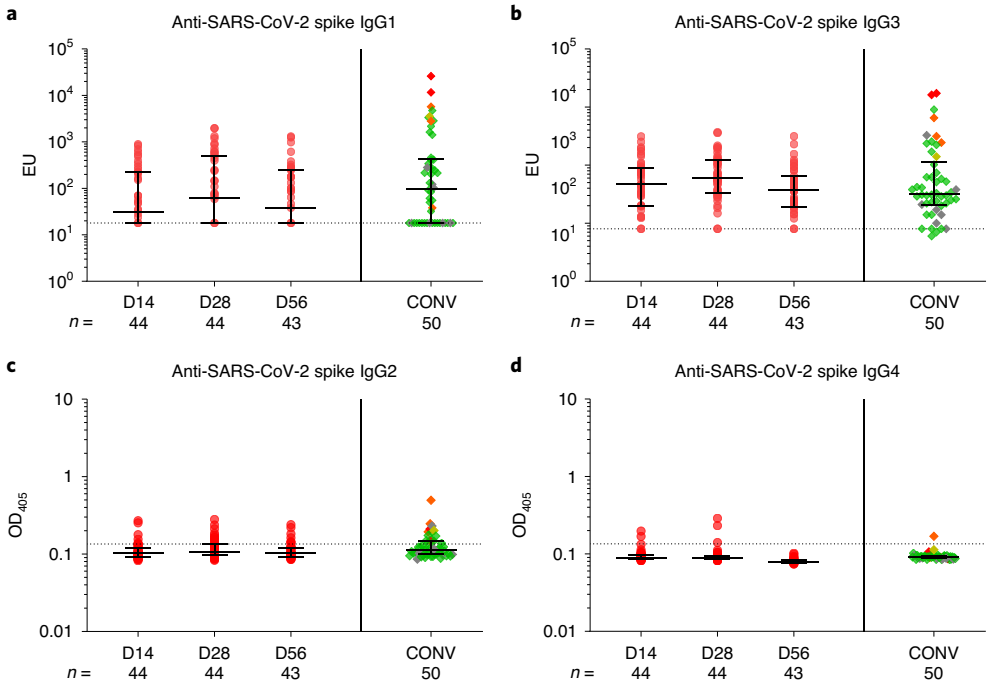

Fig. 3 | IgG subclass responses induced by ChAdOx1 nCoV-19 vaccination. Volunteers with measurable SARS-CoV-2 spike-specific IgG at day 14 were assayed for IgG subclasses. SARS-CoV-2 spike trimer-specific IgG1 (**a**) and IgG3 (**b**) responses were quantified by standardized ELISA and expressed as ELISA units (EU). IgG2 (**c**) and IgG4 (**d**) were measured by indirect ELISA and expressed as OD_{405}. Individual data points are shown here as an aligned dot plot with lines showing the median with IQR. Assays were performed at D14, D28 and D56 after vaccination ($n = 44$ for all time points, except for D56 where there were only 43 volunteers available). Dotted lines are shown at the limit of quantification of each assay. CONV, convalescent plasma samples from patients with SARS-CoV-2 who recovered are shown here as a scatter dot plot with lines showing the median with IQR ($n = 50$). CONV symbols are shown as diamonds and colored by disease severity: green, asymptomatic; gray, mildly symptomatic; yellow, moderately symptomatic; orange, severely symptomatic; and red, critically symptomatic.

positive pre-vaccination T cell and antibody responses to SARS-CoV-2 (Fig. 4f). When combinations of cytokines were assessed, few multifunctional T cells were detected in either the $CD4^+$ or $CD8^+$ T cell populations (Fig. 4g). Responses were dominated by T cells expressing single cytokines, particularly monofunctional IFN-γ^+ $CD8^+$ T cells.

Discussion

An effective vaccine against COVID-19 will likely require both neutralizing antibodies and a Th1-driven cellular component. Analyzing the induction of immune responses after vaccination is driven, in part, by concerns about enhanced disease from potentially immunopathologic Th2 responses, as seen in animal studies of vaccines against other coronaviruses[3,18–21]. Vaccine-enhanced disease was also observed in early development of inactivated vaccines against respiratory syncytial virus, wherein pathology was associated with a high ratio of non-neutralizing antibodies to neutralizing antibodies, infiltration of neutrophils and eosinophils and predominantly a Th2-biased response[32]. We showed that antibodies induced after the first dose of ChAdOx1 nCoV-19 are neutralizing and are further increased after a second dose[7] and were associated with reduced disease in vaccinated and challenged non-human primates[22].

We have described here the profile of cytokine expression from both $CD4^+$ and $CD8^+$ T cells and the IgG subclass composition of the antibody response after administration of a single dose of the ChAdOx1 nCoV-19 vaccine. Robust B cell activation and proliferation was observed after vaccination, and anti-IgA and IgG antibodies to the SARS-CoV-2 spike protein were readily detected in sera from vaccinated volunteers[7]. Anti-spike IgG responses at the peak of the response after vaccination show a polarized IgG1 response, consistent with naturally acquired antibodies against SARS-CoV-2, as well as an IgG3 response in most vaccinees. Produced early after viral infections, IgG3 coordinates multiple antibody effector functions and might contribute to recovery after SARS-CoV-2 infection[33,34]. A mixed IgG1 and IgG3 response, with low levels of IgG2 and little detectable IgG4, is in agreement with previously published reports describing the induction of Th1-type human IgG subclasses (IgG1 and IgG3) after adenoviral priming[35,36].

ChAdOx1 nCoV-19 induces a broad and robust T cell response to both S antigen subunits. The functionality of the T cell response observed here is similar in phenotype to that observed with other replication-deficient adenoviral vectors, with responses dominated by individual T cells secreting single, rather than multiple, cytokines[20]. Whether vaccine-induced monofunctional or polyfunctional T cells are of greater protective value appears to vary by disease[53,54] and is unclear for SARS-CoV-2 infection. Analysis of cytokine secretion after peptide stimulation of PBMCs demonstrated that IFN-γ and IL-2 secretion were increased in individuals who received the ChAdOx1 vaccine compared to controls, and, notably, IL-4 and IL-13 levels were not increased. Similarly, phenotyping by flow cytometry demonstrated that $CD4^+$ T cells secreted predominantly Th1 cytokines (IFN-γ, IL-2 and TNF-α) rather than Th2 (IL-5 and IL-13). Importantly, we demonstrate, with several methodologies (multiplex cytokine profiling, ICS analysis and antibody isotype profiling), that vaccination with ChAdOx1 nCoV-19 induces a predominantly Th1 response.

An important aspect in the epidemiology of COVID-19 disease is the marked difference in the mortality rates from disease between

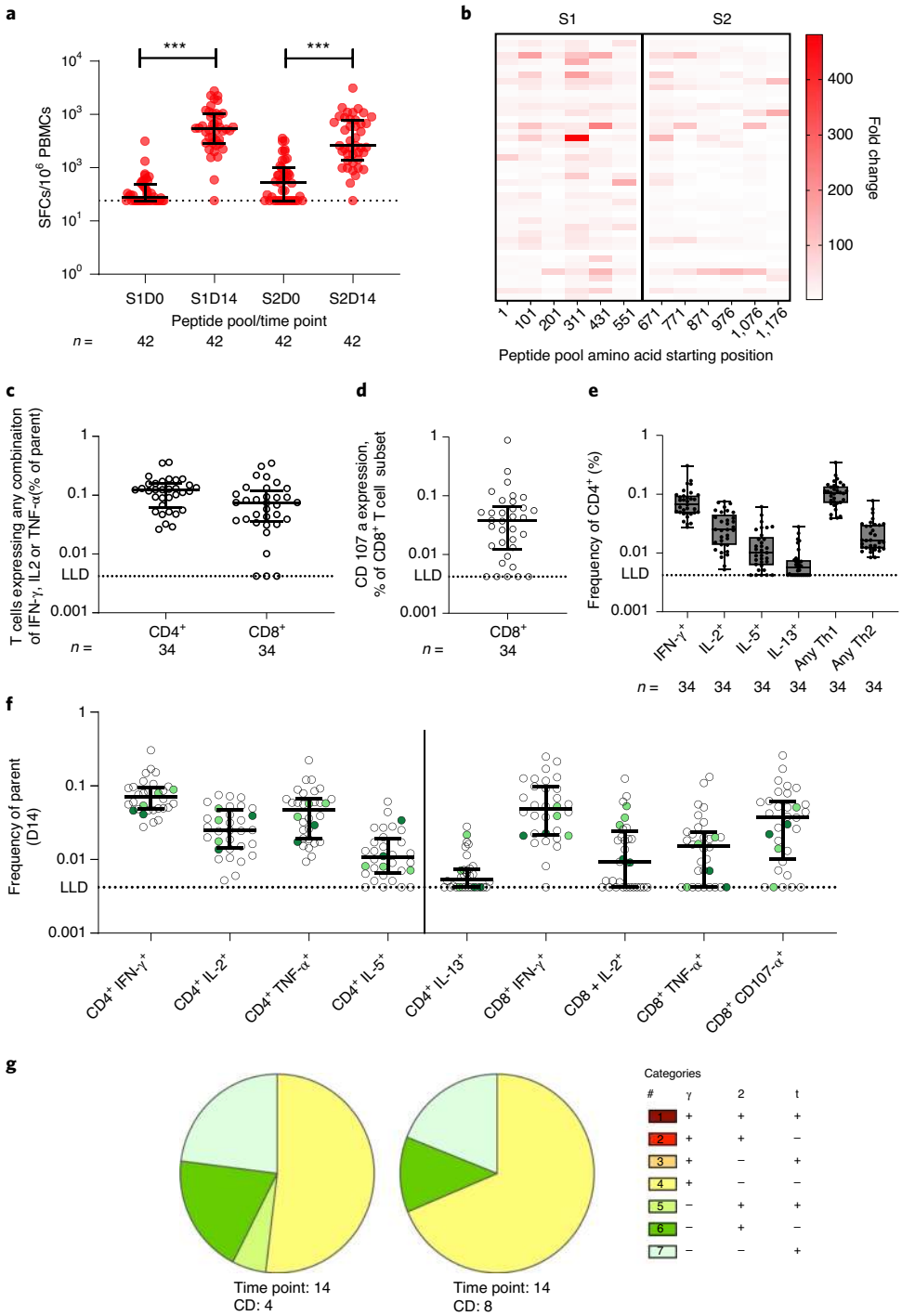

Fig. 4 | T cell responses to SARS-CoV-2 spike peptides measured by IFN-γ ELISpot and flow cytometry with ICS. Only data from individuals who received the ChAdOx1 nCoV-19 vaccine are shown. **a**, Total response to S1 and S2 (sum of six peptide pools each) at D0 and D14 after vaccination. Individual data points are shown here as a scatter dot plot with lines showing the median with IQR ($n=42$ for all time points). The dashed line represents the lower limit of detection of the assay (48 SFCs). Significant difference was determined by two-tailed Wilcoxon test (***$P<0.001$). **b**, Heat map of fold change in SFCs to each peptide pool for every participant from D0 to D14 after vaccination ($n=42$ for all time points). **c**, Frequency of CD4+ or CD8+ T cells expressing IFN-γ, IL-2 or TNF-α ($n=34$) and (**d**) frequency of CD8+ T cells expressing CD107a+ at D14 after vaccination ($n=34$). Individual data points are shown here as a scatter dot plot with lines showing the median with IQR. **e**, Frequency of Th1 and Th2 cytokine secretion by CD4+ T cells at D14 after vaccination ($n=34$). Individual data points are shown as a box plot with whiskers from the minimum to the maximum value. **f**, Frequency of CD4+ or CD8+ T cells expressing relevant individual cytokines at D14 after vaccination. Individual data points are shown here as a scatter dot plot with lines showing the median with IQR ($n=32$). Dotted lines show the lower limit of detection. Dark green circles indicate participants with an ELISpot response to the summed spike peptides pools >200 SFCs/10^6 PBMCs before vaccination ($n=2$); light green circles indicate participants with an ELISpot response to the summed spike peptides pools >200 SFCs/10^6 PBMCs who were also seropositive before vaccination ($n=3$). Clear circles represent participants with an ELISpot response <200 SFCs/10^6 PBMCs who were also seronegative before vaccination ($n=27$). **g**, Pie charts indicating the expression of cytokine combinations from CD4+ and CD8+ T cells ($n=32$, all panels). LLD, lower limit of detection.

males and females, despite similar case rates[37]. We, therefore, disaggregated the data by sex and demonstrated no difference in the magnitude of either cellular or total IgG antibody responses between male and female participants. Other significant demographic risk factors for COVID-19 disease have been shown to include age and ethnicity[38]. The sample size in this cohort was relatively small, age was limited to 18–55 years and the vast majority of participants were white, limiting the ability to investigate these variables. It will be necessary to continue disaggregated analysis of the larger phase 2 and 3 cohorts, powered for subgroup analysis. It will also be important to continue to assess immune response durability over time, with consideration given to comorbidities that might further influence vaccine-induced immunity[39].

Although there are no defined immune correlates of protection against COVID-19, it is generally accepted that high-titer neutralizing antibodies with a robust cytotoxic $CD8^+$ T cell response and Th1-biased $CD4^+$ effector response will be optimal for protective immunity after SARS-CoV-2 exposure[40]. Determining the precise threshold and phenotype of immune responses associated with protection will be crucial for bridging between populations and vaccines for any vaccine that demonstrates useful efficacy against infection or disease. If the immunogenicity of current vaccine candidates is insufficient, alternative prime-boost regimens using technologies that are rapidly and sustainably scalable, such as heterologous adenoviral prime-boost regimens, or combinations of viral vectors with approaches, such as messenger RNA (mRNA) vaccines, might be implemented. Although adenovirus-based viral vectors and mRNA vaccines have been in preclinical development for some time, few have progressed to phase 3 and subsequent market authorization; therefore, relatively little is known about effectiveness when compared to traditional vaccine platforms.

Although the number of participants studied here was relatively small, the detailed immunophenotyping of vaccine-induced immunity described here demonstrates strong humoral and cellular immune responses after a single dose, characterized by a Th1-dominated response. Importantly, several other COVID-19 vaccine candidates in clinical development have also reported neutralizing antibody responses[41] and induction of Th1-biased cell-mediated immunity.

These data further support the ongoing evaluation of the ChAdOx1 nCoV-19 vaccine candidate in phase 2 and 3 clinical trials.

Online content

Any methods, additional references, Nature Research reporting summaries, source data, extended data, supplementary information, acknowledgements, peer review information; details of author contributions and competing interests; and statements of data and code availability are available at https://doi.org/10.1038/s41591-020-01194-5.

Received: 28 October 2020; Accepted: 24 November 2020;
Published online: 17 December 2020

References

1. Draft landscape of COVID-19 candidate vaccines. https://www.who.int/publications/m/item/draft-landscape-of-covid-19-candidate-vaccines (World Health Organization, 2020).
2. de Alwis, R., Chen, S., Gan, E. S. & Ooi, E. E. Impact of immune enhancement on Covid-19 polyclonal hyperimmune globulin therapy and vaccine development. *EBioMedicine* **55**, 102768 (2020).
3. Lambert, P. H. et al. Consensus summary report for CEPI/BC March 12–13, 2020 meeting: assessment of risk of disease enhancement with COVID-19 vaccines. *Vaccine* **38**, 4783–4791 (2020).
4. McMichael, A. J., Gotch, F. M., Noble, G. R. & Beare, P. A. Cytotoxic T-cell immunity to influenza. *N. Engl. J. Med.* **309**, 13–17 (1983).
5. Del Valle, D. M. et al. An inflammatory cytokine signature predicts COVID-19 severity and survival. *Nat. Med.* **26**, 1636–1643 (2020).
6. Gudbjartsson, D. F. et al. Humoral immune response to SARS-CoV-2 in Iceland. *N. Engl. J. Med.* **383**, 1724–1734 (2020).
7. Folegatti, P. M. et al. Safety and immunogenicity of the ChAdOx1 nCoV-19 vaccine against SARS-CoV-2: a preliminary report of a phase 1/2, single-blind, randomised controlled trial. *Lancet* **396**, 467–478 (2020).
8. Marston, H. D., Paules, C. I. & Fauci, A. S. The critical role of biomedical research in pandemic preparedness. *JAMA* **318**, 1757–1758 (2017).
9. Gouglas, D., Christodoulou, M., Plotkin, S. A. & Hatchett, R. CEPI: driving progress toward epidemic preparedness and response. *Epidemiol. Rev.* **41**, 28–33 (2019).
10. Blueprint for R&D preparedness and response to public health emergencies due to highly infectious pathogens. https://www.who.int/publications/m/item/blueprint-for-r-d-preparedness-and-response-to-public-health-emergencies-due-to-highly-infectious-pathogens (World Health Organization, 2015).
11. Gilbert, S. C. & Warimwe, G. M. Rapid development of vaccines against emerging pathogens: the replication-deficient simian adenovirus platform technology. *Vaccine* **35**, 4461–4464 (2017).
12. Coughlan, L. et al. Heterologous two-dose vaccination with simian adenovirus and poxvirus vectors elicits long-lasting cellular immunity to influenza virus A in healthy adults. *EBioMedicine* **29**, 146–154 (2018).
13. Ndiaye, B. P. et al. Safety, immunogenicity, and efficacy of the candidate tuberculosis vaccine MVA85A in healthy adults infected with HIV-1: a randomised, placebo-controlled, phase 2 trial. *Lancet Respir. Med.* **3**, 190–200 (2015).
14. Sridhar, S. et al. Cellular immune correlates of protection against symptomatic pandemic influenza. *Nat. Med.* **19**, 1305–1312 (2013).
15. Peng, Y. et al. Broad and strong memory $CD4^+$ and $CD8^+$ T cells induced by SARS-CoV-2 in UK convalescent individuals following COVID-19. *Nat. Immunol.* **21**, 1336–1345 (2020).
16. Sekine, T. et al. Robust T cell immunity in convalescent individuals with asymptomatic or mild COVID-19. *Cell* **183**, 158–168 (2020).
17. Wyllie, D. et al. SARS-CoV-2 responsive T cell numbers are associated with protection from COVID-19: a prospective cohort study in keyworkers. Preprint at https://www.medrxiv.org/content/10.1101/2020.11.02.20222778v1 (2020).
18. Jackson, L. A. et al. An mRNA vaccine against SARS-CoV-2 - preliminary report. *N. Engl. J. Med.* **383**, 1920–1931 (2020).
19. Sahin, U. et al. Concurrent human antibody and TH1 type T-cell responses elicited by a COVID-19 RNA vaccine. Preprint at https://www.medrxiv.org/content/10.1101/2020.07.17.20140533v1 (2020).
20. Sadoff, J. et al. Safety and immunogenicity of the Ad26.COV2.S COVID-19 vaccine candidate: interim results of a phase 1/2a, double-blind, randomized, placebo-controlled trial. Preprint at https://www.medrxiv.org/content/10.1101/2020.09.23.20199604v1 (2020).
21. Zhu, F. C. et al. Safety, tolerability, and immunogenicity of a recombinant adenovirus type-5 vectored COVID-19 vaccine: a dose-escalation, open-label, non-randomised, first-in-human trial. *Lancet* **395**, 1845–1854 (2020).
22. van Doremalen, N. et al. ChAdOx1 nCoV-19 vaccine prevents SARS-CoV-2 pneumonia in rhesus macaques. *Nature* **586**, 578–582 (2020).
23. Barrett, J. R. et al. Phase 1/2 trial of SARS-CoV-2 vaccine ChAdOx1 nCoV-19 with a booster dose induces multifunctional antibody responses. *Nat. Med.* https://doi.org/10.1038/s41591-020-01179-4 (2021).
24. Vabret, N. et al. Immunology of COVID-19: current state of the science. *Immunity* **52**, 910–941 (2020).
25. Chen, G. et al. Clinical and immunological features of severe and moderate coronavirus disease 2019. *J. Clin. Invest.* **130**, 2620–2629 (2020).
26. Rosendahl Huber, S., van Beek, J., de Jonge, J., Luytjes, W. & van Baarle, D. T cell responses to viral infections—opportunities for peptide vaccination. *Front. Immunol.* **5**, 171 (2014).
27. Bowyer, G. et al. Reduced Ebola vaccine responses in CMV^+ young adults is associated with expansion of $CD57^+KLRG1^+$ T cells. *J. Exp. Med.* **217**, e20200004 (2020).
28. Darboe, A. et al. Enhancement of cytokine-driven NK cell IFN-γ production after vaccination of HCMV infected Africans. *Eur. J. Immunol.* **47**, 1040–1050 (2017).
29. Hammer, Q. et al. Peptide-specific recognition of human cytomegalovirus strains controls adaptive natural killer cells. *Nat. Immunol.* **19**, 453–463 (2018).
30. Wajnberg, A. et al. SARS-CoV-2 infection induces robust, neutralizing antibody responses that are stable for at least three months. Preprint at https://www.medrxiv.org/content/10.1101/2020.07.14.20151126v1 (2020).
31. Alharbi, N. K. et al. ChAdOx1 and MVA based vaccine candidates against MERS-CoV elicit neutralising antibodies and cellular immune responses in mice. *Vaccine* **35**, 3780–3788 (2017).
32. Jorquera, P. A., Anderson, L. & Tripp, R. A. Understanding respiratory syncytial virus (RSV) vaccine development and aspects of disease pathogenesis. *Expert Rev. Vaccines* **15**, 173–187 (2016).
33. Atyeo, C. et al. Distinct early serological signatures track with SARS-CoV-2 survival. *Immunity* **53**, 524–532 (2020).

34. Addetia, A. et al. Neutralizing antibodies correlate with protection from SARS-CoV-2 in humans during a fishery vessel outbreak with a high attack rate. *J. Clin. Microbiol.* **58**, JCM.02107–02120 (2020).
35. Hodgson, S. H. et al. Combining viral vectored and protein-in-adjuvant vaccines against the blood-stage malaria antigen AMA1: report on a phase 1a clinical trial. *Mol. Ther.* **22**, 2142–2154 (2014).
36. Barouch, D. H. et al. Evaluation of a mosaic HIV-1 vaccine in a multicentre, randomised, double-blind, placebo-controlled, phase 1/2a clinical trial (APPROACH) and in rhesus monkeys (NHP 13-19). *Lancet* **392**, 232–243 (2018).
37. Bhopal, S. S. & Bhopal, R. Sex differential in COVID-19 mortality varies markedly by age. *Lancet* **396**, 532–533 (2020).
38. Wolff, D., Nee, S., Hickey, N. S. & Marschollek, M. Risk factors for Covid-19 severity and fatality: a structured literature review. *Infection* https://doi.org/10.1007/s15010-020-01509-1 (2020).
39. The gendered dimensions of COVID-19. *Lancet* **395**, 1168 (2020).
40. Jeyanathan, M. et al. Immunological considerations for COVID-19 vaccine strategies. *Nat. Rev. Immunol.* **20**, 615–632 (2020).
41. Mulligan, M. J. et al. Phase I/II study of COVID-19 RNA vaccine BNT162b1 in adults. *Nature* **586**, 589–593 (2020).

the Oxford COVID Vaccine Trial Group

Aabidah Ali[1], Elizabeth Allen[1], Megan Baker[1], Eleanor Barnes[1], Nicola Borthwick[1], Amy Boyd[1], Charlie Brown-O'Sullivan[1], Joshua Burgoyne[1], Nicholas Byard[1], Ingrid Cabrera Puig[1], Federica Cappuccini[1], Jee-Sun Cho[1], Paola Cicconi[1], Elizabeth Clark[1], Wendy E. M. Crocker[1], Mehreen S. Datoo[1], Hannah Davies[1], Francesca R. Donnellan[1], Susanna Jane Dunachie[1], Nick J. Edwards[1], Sean C. Elias[1], Jamie Fowler[1], Julie Furze[1], Ciaran Gilbride[1], Giacomo Gorini[1], Gaurav Gupta[1], Stephanie A. Harris[1], Susanne H. C. Hodgson[1], Mimi M. Hou[1], Susan Jackson[1], Kathryn Jones[1], Reshma Kailath[1], Lloyd King[1], Colin W. Larkworthy[1], Yuanyuan Li[1], Amelia M. Lias[1], Aline Linder[1], Samuel Lipworth[1], Raquel Lopez Ramon[1], Meera Madhavan[1], Rebecca Makinson[1], Emma Marlow[1], Julia L. Marshall[1], Alexander J. Mentzer[1], Hazel Morrison[1], Nathifa Moya[1], Ekta Mukhopadhyay[1], Andrés Noé[1], Fay L. Nugent[1], Dimitra Pipini[1], David Pulido-Gomez[1], Fernando Ramos Lopez[1], Adam John Ritchie[1], Indra Rudiansyah[1], Stephannie Salvador[1], Helen Sanders[1], Iman Satti[1], Adam Shea[1], Sarah Silk[1], Alexandra J. Spencer[1], Rachel Tanner[1], Iona Jennifer Taylor[1], Yrene Themistocleous[1], Merin Thomas[1], Nguyen Tran[1], Adam Truby[1], Cheryl Turner[1], Nicola Turner[1], Marta Ulaszewska[1], Andrew T. Worth[1], Lucy Kingham-Page[1], Marco Polo Peralta Alvarez[1], Rachel Anslow[2], Louise Bates[2], Kirsten Beadon[2], Rebecca Beckley[2], Amy Beveridge[2], Else Margreet Bijker[2], Luke Blackwell[2], Jamie Burbage[2], Susana Camara[2], Melanie Carr[2], Irina Chelysheva[2], Rachel Colin-Jones[2], Rachel Cooper[2], Christina J. Cunningham[2], Tesfaye Demissie[2], Claudio Di Maso[2], Naomi Douglas[2], Rachael Drake-Brockman[2], Ruth Elizabeth Drury[2], Katherine R. W. Emary[2], Sally Felle[2], Shuo Feng[2], Carla Ferreira Da Silva[2], Karen J. Ford[2], Emma Francis[2], Lara Gracie[2], Joseph Hamlyn[2], Brama Hanumunthadu[2], Daisy Harrison[2], Thomas C. Hart[2], Sophia Hawkins[2], Jennifer Hill[2], Elizabeth Howe[2], Nicola Howell[2], Elizabeth Jones[2], Jade Keen[2], Sarah Kelly[2], David Kerr[2], Liaquat Khan[2], Jasmin Kinch[2], Stanislava Koleva[2], Emily A. Lees[2], Alice Lelliott[2], Xinxue Liu[2], Natalie G. Marchevsky[2], Spyridoula Marinou[2], Joanne McEwan[2], Ella Morey[2], Gertraud Morshead[2], Jilly Muller[2], Claire Munro[2], Sarah Murphy[2], Philomena Mweu[2], Elizabeth Nuthall[2], Katie O'Brien[2], Daniel O'Connor[2], Peter John O'Reilly[2], Blanché Oguti[2], Piper Osborne[2], Nelly Owino[2], Kaye Parker[2], Katja Pfafferott[2], Daniel Phillips[2], Samuel Provstgaard-Morys[2], Helen Ratcliffe[2], Thomas Rawlinson[2], Sarah Rhead[2], Hannah Roberts[2], Katherine Sanders[2], Laura Silva-Reyes[2], Christine S. Rollier[2], Catherine C. Smith[2], David J. Smith[2], Lisa Stockdale[2], Anna Szigeti[2], Tonia M. Thomas[2], Amber Thompson[2], Adriana Tomic[2], Susan Tonks[2], Rachel Varughese[2], Marije K. Verheul[2], Iason Vichos[2], Laura Walker[2], Caroline White[2], Rachel White[2], Xin Li Yao[2], Christopher P. Conlon[3], John Frater[3], Liliana Cifuentes[4], Ioana Baleanu[5], Emma Bolam[5], Elena Boland[5], Tanja Brenner[5],

Brad E. Damratoski[5], Chandra Datta[5], Omar El Muhanna[5], Richard Fisher[5], Pablo Galian-Rubio[5], Gina Hodges[5], Frederic Jackson[5], Shuchang Liu[5], Lisa Loew[5], Roisin Morgans[5], Susan Jane Morris[5], Vicki Olchawski[5], Catarina Oliveria[5], Helena Parracho[5], Emilia Reyes Pabon[5], Abdessamad Tahiri-Alaoui[5], Keja Taylor[5], Paul Williams[5], Dalila Zizi[5], Edward H. Arbe-Barnes[6], Philip Baker[6], Alexander Batten[6], Charlotte Downing[6], Jonathan Drake[6], Marcus Rex English[6], John Aaron Henry[6], Poppy Iveson[6], Annabel Killen[6], Thomas B. King[6], Jessica P. J. Larwood[6], Garry Mallett[6], Kushal Mansatta[6], Neginsadat Mirtorabi[6], Maia Patrick-Smith[6], James Perring[6], Kajal Radia[6], Sophie Roche[6], Ella Schofield[6], Rebecca te Water Naude[6], James Towner[6], Natalie Baker[7], Kevin R. Bewley[7], Emily Brunt[7], Karen R. Buttigieg[7], Miles W. Carroll[7], Sue Charlton[7], Naomi S. Coombes[7], Michael J. Elmore[7], Kerry Godwin[7], Bassam Hallis[7], Daniel Knott[7], Lorna McInroy[7], Imam Shaik[7], Kelly Thomas[7], Julia A. Tree[7], Caitlin L. Blundell[8], Michelangelo Cao[9], Dearbhla Kelly[9], Annina Schmid[9], Donal T. Skelly[9], Andreas Themistocleous[9], Tao Dong[10], Samantha Field[11], Elizabeth Hamilton[11], Elizabeth Kelly[12], Paul Klenerman[13], Julian C. Knight[14], Yolanda Lie[15], Christos Petropoulos[15], Cynthia Sedik[15], Terri Wrin[15], Gretchen Meddaugh[16], Yanchun Peng[13], Gavin Screaton[6] and Elizabeth Stafford[17]

[6]Medical Sciences Division, University of Oxford Medical School, University of Oxford, Oxford, UK. [7]National Infection Service, Public Health England, Oxford, UK. [8]Department of Biochemistry, University of Oxford, Oxford, UK. [9]Nuffield Department of Clinical Neurosciences, University of Oxford, Oxford, UK. [10]Chinese Academy of Medical Sciences Oxford Institute, Nuffield Department of Medicine, Oxford University, Oxford, UK. [11]Nuffield Department of Population Health, University of Oxford, Oxford, UK. [12]Clinical Virology, AstraZeneca, Washington, DC, UK. [13]NDM Experimental Medicine, University of Oxford, Oxford, UK. [14]Wellcome Trust Centre for Human Genetics, University of Oxford, Oxford, UK. [15]Monogram Biosciences LabCorp, San Francisco, CA, USA. [16]Human Tissue Governance Team, Research Services, University of Oxford, Oxford, UK. [17]Oxford University Hospitals NHS Foundation Trust, Oxford, UK.

Methods

Study procedures and sample processing. Full details on the conduct of the phase 1/2 randomized controlled trial of ChAdOx1 nCoV-19 (AZD1222), including the trial protocol, were previously published[7]. This study was registered at ISRCTN (15281137) and ClinicalTrials.gov (NCT04324606). Only data from single-dose vaccinated volunteers are included in this paper. Before enrolment, all participants gave written informed consent. The trial was conducted according to the principles of Good Clinical Practice, and approval was obtained from a national ethics committee (South Central Berkshire Research Ethics Committee, reference 20/SC/0145) and a regulatory agency in the United Kingdom (the Medicines and Healthcare Products Regulatory Agency). An independent data safety monitoring board was appointed before recruitment began.

Blood samples were collected on the day of vaccination and 7, 14, 28 and 56 d after vaccination. At time points for immunological analyses, blood samples were taken in both plain and heparinized collection tubes. Samples were processed within 4 h of the blood draw. Plain tubes were processed for the collection of blood serum. Tubes were centrifuged at 1,800 r.p.m. for 5 min, and the serum was harvested for storage at −80 °C until required. Heparinized tubes were processed for the collection of PBMCs and blood plasma by density gradient centrifugation. Blood was decanted into Leucosep tubes (Greiner Bio-One) containing Lymphoprep (STEMCELL Technologies) and centrifuged at 1,000*g* for 13 min with the brake off. A fraction of blood plasma was collected and stored at −80 °C, while the remaining sample was decanted into a fresh Falcon tube and topped up with R0 media (RPMI-1640 cell culture media containing 1% penicillin–streptomycin and 2 mM L-glutamine (all Sigma-Aldrich). Samples were centrifuged again at 1,800 r.p.m. for 5 min; the supernatant was poured off; and the cell pellet was resuspended once more in R0 media for washing. After centrifugation, the cell pellet was resuspended in 10 ml of R10 media (RPMI-1640 containing 1% penicillin–streptomycin, 2 mM L-glutamine and 10% fetal calf serum (FCS, Labtech) for counting.

Cells were counted using a CasyCounter (OMNI Life Science) for use in fresh assays or for cryopreservation. The assays performed on fresh cells were ELISpot and ICS only (described below). All remaining cells were frozen at a concentration of 8–12 × 10^6 PBMCs per ml. After centrifugation (1800 r.p.m., 5 min) cells were resuspended in cold FCS at half the total freeze-down volume. Cells were placed in a refrigerator (2–8 °C) for 20 min before an equal volume of cold FCS containing 20% dimethylsulphoxide was added. One-milliliter aliquots were prepared and quickly transferred to CoolCells (Corning) for freezing at −80 °C overnight. Tubes were then transferred to a −150 °C ultra-low temperature freezer until required.

Convalescent plasma samples were obtained from hospitalized adult (≥18 years) patients admitted with polymerase chain reaction-positive SARS-CoV-2 infection or from healthcare workers enrolled in COVID-19 surveillance studies. Studies were approved by the following committees: Gastrointestinal Illness in Oxford: COVID substudy (Sheffield Research Ethics Committee, reference 16/YH/0247); ISARIC/WHO Clinical Characterisation Protocol for Severe Emerging Infections (Oxford Research Ethics Committee C, reference 13/SC/0149); and Sepsis Immunomics Project (Oxford Research Ethics Committee C, reference 19/SC/0296). Both asymptomatic and symptomatic participants were tested for each assay. Additional details on experimental procedures performed on convalescent plasma samples were described previously[7].

Peptides and stimulations. Peptides spanning the full length of the SARS-CoV-2 spike protein sequence were synthesised for use in antigen-specific T cell assays (ProImmune). A total of 253 peptides were synthesized as 15-mers overlapping by ten amino acids. Peptides were also synthesized for the N-terminal tPA leader sequence, which was included to increase expression of the vaccine antigen from the adenoviral vector. Details of peptide sequences and pooling for assays are shown in Supplementary Table 3. Briefly, for the Cytek Aurora flow cytometry assay, Meso Scale Discovery (MSD) Th1/Th2 cytokine profiling assay and ICS, two separate peptide pools were made spanning the S1 (134 peptides) and S2 (119 peptides) subunits of the SARS-CoV-2 spike protein. For the ELISpot assay, 12 pools of 18–24 peptides were made consisting of six pools each for the S1 and S2 subunits. A separate tPA leader sequence pool (five peptides) was included in this assay.

Flow cytometry conducted on a Cytek Aurora spectral analyzer. Flow cytometry was performed from frozen aliquots of PBMCs of donors from days 0, 7, 14 and 28 after vaccination with ChAdOx1 nCoV19 (D0 $n=24$, D7 $n=23$, D14 $n=25$ and D28 $n=24$). Cells were defrosted in media containing >5 U ml^{-1} of benzonase and resuspended in complete RPMI media supplemented with 10% FCS, L-glutamine and penicillin–streptomycin at a concentration of 2 × 10^7 cells per ml. Then, 2 × 10^6 PBMCs per well were plated in a 96-well plate and stimulated with synthetic peptides spanning the SARS-CoV-2 spike protein split into two separate pools for the S1 and S2 subunits (Supplementary Table 3) at a final concentration of 2 μg ml^{-1} or media as a control. One well per donor was stimulated with phorbol 12-myristate 13-acetate and ionomycin (Cell Activation Cocktail, BioLegend) as a positive control. PBMCs were co-stimulated in the presence of anti-human CD28, CD49d (1 μg ml^{-1}; Life Technologies) and CD107a-BV785 (BioLegend) for 2 h at 37 °C with 5% CO_2 and then incubated for an additional 16 h after the addition of 1 μg ml^{-1} of brefeldin A and monensin to each well (BioLegend).

PBMCs were washed in FACS buffer (phosphate-buffered saline with 0.5% bovine serum albumin and 1% EDTA) and stained with a cocktail of surface antibodies, including anti-human Live/Dead-Zombie UV, CD4-AF700, CD19-Spark NIR 685, CD56-APC, CCR7-PerCP/Cy5.5, PD1-PE/Dazzle 594, CD57-PE/Cy7(BioLegend) CD8-AF405, CD45RA-SuperBright 702, CD27-PerCP eF710 and CD20-AF532 (Thermo Fisher Scientific); CD16-BUV495, CD3-BUV661, CD138-BUV805, NKG2A-BV480 and IgM-BB515 (BD Biosciences); and NKG2C-PE and KLRG1-VioBlue (Miltenyi) in FACS buffer with 10% Brilliant Stain Buffer Plus (BD Biosciences). PBMCs were incubated at 4 °C in the dark for 30 min and then washed twice in FACS buffer. PBMCs were then incubated in CytoFix/CytoPerm solution (BD Biosciences) at 4 °C in the dark for 30 min and then washed twice in Perm/Wash buffer and then stained with a cocktail of intracellular antibodies, including anti-human IFN-γ-BV650 and IL-2-BV605 (BioLegend); IgG-BV421, TNF-α-BUV395, CD69-BV750, CD71-BUV563 and CD25-BV737 (BD Biosciences); and Ki-67-APC eF780 (Thermo Fisher Scientific) in Perm/Wash. PBMCs were incubated at 4 °C in the dark for 30 min, washed twice in Perm/Wash buffer, once in FACS buffer and then re-suspended in 200 μl of FACS buffer for acquisition on a custom four-laser Cytek Aurora spectral analyzer using SpectroFlo v2.2 (Cytek Biosciences).

Single-fluorochrome compensation was calculated on beads (BD Biosciences and Miltenyi) or human PBMCs. Analysis of data was conducted in FlowJo (v10.6.2) by a hierarchical gating strategy (Supplementary Fig. 6) and Prism 8 (GraphPad). Peptide-specific responses were calculated by subtraction of the unstimulated controls from the peptide-stimulated samples.

Downsampling and tSNE analysis were conducted on gated live lymphocytes in FlowJo v.10.7.1. A random sample of 100,000 cells per donor and time point was collected and concatenated into a single file. All fluorochrome colors and the sample time point were included as parameters. The tSNE analysis was implemented in FlowJo v.10.7.1 with 100,000 iterations and a perplexity of 30 and using Barnes–Hut gradient algorithm.

MSD Th1/Th2 cytokine profiling. Th1/Th2 cytokine responses were measured in tissue culture supernatants from the stimulation of PBMCs with synthetic peptides covering the spike protein. Then, 5 × 10^5 freshly isolated PBMCs were resuspended in 250 μl of R10 media in 96-well U-bottom plates and supplemented with 1 μg ml^{-1} of anti-human CD28 and CD49d. Peptides spanning the S1 and S2 subunits of the SARS-CoV-2 spike protein (Supplementary Table 3) were added to separate wells at a concentration of 2 μg ml^{-1}. Each sample also included an unstimulated (media-only) control. After a 16–18-h incubation at 37 °C with 5% CO_2, cells were pelleted by centrifugation (1,800 r.p.m., 5 min), and 200 μl of supernatant was harvested. Supernatants from the S1 and S2 stimulations were combined and stored at −80 °C until required.

Cytokine responses were analyzed using the MSD V-PLEX Proinflammatory Cytokine (human) Panel 1 Kit, validated by MSD. Each plate is coated with nine different capture monoclonal antibodies against nine different cytokines arranged in independent spots on the base of each well. Cytokines IFN-γ, IL-1β, IL-2, IL-4, IL-8, IL-10, IL-12p70, IL-13 and TNF-α were associated with either a Th1- or Th2-type T cell response.

Supernatants were diluted 1:2 for unstimulated samples and 1:10 for S1/S2 stimulated samples in MSD Diluent 2. The kit provides a multi-analyte lyophilized calibrator that, when reconstituted, will be used as the standard curve using a four-fold serial dilution to form an eight-point standard curve plated out in duplicate. Cytokine measurements were carried out according to the manufacturer's instructions. Plates were read on an MSD reader within 15 min of adding the read buffer.

Data were analyzed using MSD Discovery Workbench 4.0. Samples were repeated if any sample had a replicate with a coefficient of variation greater than 20%. Replicates were read off the standard curve and multiplied by the dilution factor, and concentration was reported as the average of the replicates in pg ml^{-1}. Concentration from unstimulated sample was subtracted from concentration from stimulated (background subtract). Negative values of background subtracts were replaced by zeros. An arbitrary value of 0.0001 was added to the background subtracts across all the samples to overcome the presence of null values raised from samples too low to be read off the standard curve.

Isotype and subclass standardized ELISA. Samples from participants vaccinated with ChAdOx1 nCoV-19 and convalescent plasma samples were assayed for anti-spike IgG1, IgG3, IgA and IgM. Samples from participants vaccinated with MenACWY were assayed for anti-spike IgA and IgM antibodies only. Standardized ELISA was used to quantify circulating SARS-CoV-2 spike-specific IgG1, IgG3, IgA and IgM responses. Full methodological details for this assay were previously published[23]. Briefly, ELISA plates were coated overnight with 5 μg ml^{-1} of SARS-CoV-2 full-length spike protein. After blocking with Blocker Casein in PBS (Thermo Fisher Scientific), samples (minimum 1:50 dilution) were incubated for 2 h at 37 °C with 300 r.p.m. shaking. Standard curve and internal controls were created from reference serum using a pool of high-titer donor serum. An alkaline phosphatase-conjugated secondary antibody (dependent on the immunoglobulin subclass or isotype being detected) was then added and incubated for 1 h at 37 °C with 300 r.p.m. shaking. Plates were developed using PNPP alkaline phosphatase

substrate (Thermo Fisher Scientifc) for 1–4 h at 37 °C with 300 r.p.m. shaking and read at 405 nm when the internal control reached an OD_{405} of 1. Plate pass/fail criteria are described in ref. [23].

Isotype and subclass optical density ELISA. Antigen-specific IgG2, IgG4 and IgE responses were detected in the absence of an antigen-specific serum control by optical density (OD) ELISA. Detailed procedures for this assay were previously described[23]. Briefly, ELISA plates were coated overnight with 5 μg ml^{-1} of SARS-CoV-2 full-length spike protein, plus a commercial human immunoglobulin control for the antibody isotype or subclass being assayed. After blocking with Blocker Casein in PBS, test samples and pre-pandemic negative controls (minimum 1:50 dilution) were plated out for 2 h at 37 °C with 300 r.p.m. shaking. Different alkaline phosphatase-conjugated secondary antibodies were added depending on the immunoglobulin isotype or subclass being assayed for 1 h at 37 °C with 300 r.p.m. shaking. Plates were developed using PNPP alkaline phosphatase substrate for 1–4 h at 37 °C with 300 r.p.m. shaking and read at 405 nm when the immunoglobulin control reached a specified OD_{405}. Negative cutoff calculations are described in ref. [23].

Avidity ELISA. The avidity of SARS-CoV-2 spike-specific IgG from volunteers who had a quantifiable response at day 28 was assessed. Anti-SARS-CoV-2 spike-specific total IgG antibody avidity of donor serum was assessed by sodium thiocyanate (NaSCN)-displacement ELISA. Nunc MaxiSorp ELISA plates (Thermo Fisher Scientific) were coated overnight (≥16 h) at 4 °C with 50 μl per well of 2 μg ml^{-1} of SARS-CoV-2 trimeric spike protein diluted in PBS. Plates were washed three times with PBS/Tween (0.05%) (PBS/T) and tapped dry. Plates were blocked for 1 h with 100 μl per well of Blocker Casein in PBS (Thermo Fisher Scientific) at 20 °C. Test samples and a positive control serum pool were diluted in blocking buffer to normalize them to an OD_{405} of 1, and 50 μl per well was added in duplicate to each row of the plate (except the last row, where only blocking buffer was added). Plates were incubated for 2 h at 20 °C and then washed three times with PBS/T and tapped dry. Increasing concentrations of NaSCN (Sigma-Aldrich) diluted in PBS were added at 50 μl per well to each row down the plate (1 M, 2 M, 3 M, 4 M, 5 M and 6 M) except for the first and last row, where only PBS was added. Plates were incubated for 15 min at 20 °C and then washed six times with PBS/T and tapped dry. Anti-human IgG (γ-chain specific) alkaline phosphatase antibody produced in goat (Sigma-Aldrich) was diluted 1:1,000 in blocking buffer, and 50 μl per well was added to the plate. Plates were incubated for 1 h at 20 °C and then washed three times with PBS/T and tapped dry. Then, 100 μl per well of PNPP alkaline phosphatase substrate (Thermo Fisher Scientific) was added, and plates were incubated at 20 °C. OD at 405 nm (OD_{405}) was measured using an ELx808 absorbance reader (BioTek) until the untreated sample wells reached an OD_{405} of 1 (0.8–2.0). Gen5 ELISA software v3.09 (BioTek) was used to plot the test sample OD_{405} against concentration of NaSCN, and a spline function with smoothing factor 0.001 was fitted to the data. For each sample, concentration of NaSCN required to reduce the OD_{405} to 50% of that without NaSCN (IC_{50}) was interpolated from this function and reported as a measure of avidity.

Ex vivo IFN-γ ELISpot assays. ELISpot assays were performed on freshly isolated PBMCs before and 14 d after vaccination with ChAdOx1 nCoV19, as previously described[7]. Assays were performed using Multiscreen IP ELISpot plates (Millipore) and were coated overnight at 4 °C with 10 μg ml^{-1} of human anti-IFN-γ coating antibody (clone 1-D1K, Mabtech) in carbonate buffer, before washing three times with PBS and blocking with R10 media for 2–8 h. Then, 2.5×10^5 PBMCs were added to each well of the plate, along with 13 pools of peptides covering the SARS-CoV-2 spike protein and the N-terminal tPA leader sequence at a final concentration of 10 μg ml^{-1} (Supplementary Table 3). Each assay was performed in triplicate and incubated for 16–18 h at 37 °C with 5% CO_2.

Plates were then developed by washing six times with PBS/T, followed by the addition of 1 μg ml^{-1} of anti-IFN-γ detector antibody (7-B6-1-Biotin) to each well. After a 2–4-h incubation, plates were washed again, and 1:1,000 SA-ALP was added for 1–2 h. After a final wash step, plates were developed using BCIP NBT-plus chromogenic substrate (Moss).

ELISpot plates were counted using an AID automated ELISpot counter (AID Diagnostika, algorithm C), using identical settings for all plates, and spot counts were adjusted only to remove artifacts. Responses were averaged across triplicate wells, and the mean response of the unstimulated (negative control) wells was subtracted. Results are expressed as SFCs/10^6 PBMCs. Responses to a peptide were considered positive if background subtracted responses were >40 SFUs/10^6 PBMCs. If responses were >80 SFCs/10^6 PBMCs in the negative control wells (PBMCs without antigen) or <800 SFCs/10^6 PBMCs in the positive control wells (pooled *Staphylococcal enterotoxin* B at 0.02 μg ml^{-1} and phytohaemagglutinin-L at 10 μg ml^{-1}), results were excluded from further analysis.

ICS. ICS was performed on freshly isolated PBMCs stimulated with pooled S1 and S2 peptides. Then, 3×10^6 PBMCs were resuspended in 5 ml of polypropylene FACS tubes to a volume of 1 ml in R10 media supplemented with 1 μg ml^{-1} of anti-human CD28 and CD49d and 1 μl of CD107a PE-Cy5 (eBioscience). S1 and S2 peptide pools (Supplementary Table 3) were added at a concentration of 2 μg ml^{-1}. Each sample also included a positive control (*S. enterotoxin* B at 1 μg ml^{-1}; Sigma Aldrich) and an unstimulated (media-only) control. Cells were incubated at 37 °C with 5% CO_2 for 16–20 h, with brefeldin A (3 μg ml^{-1}) and monensin (2 mM) (eBioscience) added after 2 h

At the end of the incubation, cells were washed in FACS buffer (PBS containing 0.1% bovine serum albumin and 0.01% NaN_3) and transferred to a 96-well U-bottom tissue culture plate for staining. A surface staining cocktail was first added containing 2.5 μl of a 1:40 dilution of Aqua Live/Dead stain (Thermo Fisher Scientific) and 1 μl of BV711 CCR7 (BioLegend) in 46.5 μl of FACS buffer. Cells were incubated in the dark for 20 min and washed with FACS buffer. Then, 100 μl of CytoFix/CytoPerm solution (BD Biosciences) was added to each well and left to incubate for an additional 20 min. Cells were then washed with Perm/Wash buffer before ICS. The ICS cocktail contained 0.025 μl of CD45RA BV605, 0.025 μl of TNF-α PE-Cy7, 0.1 μl of IFN-γ FITC, 0.025 μl of CD14 e450, 0.025 μl of CD19 e450, 0.5 μl of CD3 AF700, 1 μl of IL-2 BV650, 1.25 μl of IL-5 PE, 2.5 μl of IL-13 APC, 3.5 μl of CD4 PerCP Cy5.5 and 5 μl of CD8 APC-eF780, to a total volume of 50 μl diluted in FACS buffer. Samples were stained in the dark for 30 min. Cells were washed twice with Perm/Wash buffer and twice with FACS buffer before being resuspended in 100 μl of 1% paraformaldehyde.

Compensation controls were prepared fresh for each batch using OneComp eBeads (eBioscience). Cells were kept on ice and strained through a 35-μm filter before acquisition. Cells were acquired on a five-laser BD LSRFortessa flow cytometer (BD Biosciences) using FACSDiva v8.02 (BD Biosciences), and data were analyzed in FlowJo v10.7. A hierarchical gating strategy was applied for sample analysis (Supplementary Fig. 7). A quality control process was applied to remove samples with fewer than 100,000 events in the live $CD3^+$ gate and samples with <1% cytokine response to *S. enterotoxin* B ($CD4^+$ and $CD8^+$ IFN-γ^+, $CD8^+$ TNF-α^+). A lower limit of detection was applied, and only samples with an ELISpot response greater than 200 SFCs/10^6 PBMCs were included in the analysis.

Statistical analysis. All statistical tests, as well as all graphical representation of the data, were performed in GraphPad Prism 8.4.3. Data are presented as medians with IQRs. To check for the normality of the data, d'Agostino–Pearson tests were used. Unpaired samples were compared using Mann–Whitney U tests, and paired samples were compared with the Wilcoxon test. All tests were two tailed, with a 5% per-comparison error rate. Bonferroni correction was used to correct for multiple comparisons. Correlations were analyzed using Spearman's rank test. *P* values less than 0.05 were considered significant.

Reporting Summary. Further information on research design is available in the Nature Research Reporting Summary linked to this article.

Data availability

The University of Oxford is committed to providing access to anonymized data for non-commercial research at the end of the clinical trial, which is currently scheduled to be 1 year after the last participant is enrolled, unless granted an extension. Oxford will collaborate with AstraZeneca UK on such requests before disclosure.

Acknowledgements

This work was funded by UK Research and Innovation (MC_PC_19055); the Engineering and Physical Sciences Research Council (EP/R013756/1); the Coalition for Epidemic Preparedness Innovations (CEPI); and the National Institute for Health Research (NIHR) and the NIHR Oxford Biomedical Research Centre. Additional resources for study delivery were provided by the NIHR Southampton Clinical Research Facility and the NIHR Southampton Biomedical Research Centre; University Hospital Southampton NHS Foundation Trust; the NIHR Imperial Clinical Research Facility; and the NIHR North West London, South London, Wessex and West of England Local Clinical Research Networks and the NIHR Oxford Health Biomedical Research Centre. P.M.F. received funding from the Coordenacao de Aperfeicoamento de Pessoal de Nivel Superior, Brazil (finance code 001). Development of SARS-CoV-2 reagents was partially supported by the U.S. National Institute of Allergy and Infectious Diseases Centers of Excellence for Influenza Research and Surveillance contract HHSN272201400008C. The research reagent for SARS-CoV-2 RNA (NIBSC 20/130) was obtained from the National Institute for Biological Standards and Control, UK. The control vaccine was provided free of charge by the UK Department of Health and Social Care. We received invaluable additional financial support through generous philanthropic donations to the University of Oxford, including from the Huo Family Foundation. The University of Oxford has entered into a partnership with AstraZeneca for further development of ChAdOx1 nCov-19 (AZD1222). The authors are grateful to the senior management at AstraZeneca for facilitating and funding the manufacture of the AZD1222 vaccine candidate, the pseudovirus neutralization assays and the Meso Scale antibody assay used in this study. AstraZeneca reviewed the data from the study and the final manuscript before submission, but the authors retained editorial control. The investigators express their gratitude for the contribution of all the trial participants, the invaluable advice of the international Data Safety Monitoring Board (R. Heyderman, M. Sadarangani, S. Black, G. Bouliotis, G. Hussey, B. Ogutu, W. Orenstein, S. Ramos, C. Dekker and E. Bukusi) and the independent members of the Trial Steering Committee. We additionally acknowledge the broader support from the various teams within the University of Oxford, including the Medical Sciences Division, the Nuffield

Department of Medicine (R. Cornall and O. Velicka) and the Department of Paediatrics (G. A. Holländer, J. Bagniewska, E. Derow and S. Vanderslott), the Oxford Immunology Network COVID Consortium, Clinical Trials Research Governance (H. House, C. Riddle, R. Bahadori and A. Brindle), Research Services (C. Banner and S. Pelling-Deeves), the Public Affairs Directorate (J. Colman, A. Buxton, C. McIntyre and S. Pritchard) and the Clinical Biomanufacturing Facility, as well as the Oxford University Hospitals NHS Foundation Trust (B. Holthof) and the Oxford Health NHS Foundation Trust and the trial sites. We are grateful for the input of the protein production team at the Jenner Institute. The MSD Quickplex was purchased using joint support from Versus Arthritis (grant reference 21509), Wellcome MSD ISSF (BRD00010) and the Kennedy Trust for Rheumatology Research. The views expressed in this publication are those of the authors and not necessarily those of the NIHR or the UK Department of Health and Social Care, UK Research and Innovation, Coalition for Epidemic Preparedness Innovations, the National Institute for Health Research, the NIHR Oxford Biomedical Research Centre, Thames Valley and South Midland's NIHR Clinical Research Network or AstraZeneca. A.F.'s post was supported by the Chinese Academy of Medical Sciences Innovation Fund for Medical Science, China (grant number 2018-I2M-2-002).

Author contributions

Conceived and designed experiments: A.F., K.E., T.L. and H.S. Methodology: S.B.-R., J.B. and K.E. Formal analysis: S.B.-R., J.B., H.S., A.F., I.C., R.A.M., R.I.M., K.E., D.B. and M.V. Investigation: S.B.-R., J.B., R.M., H.S., R.A.M., R.I.M., K.E., D.B., J.A., N.P., S.S., J.A., J.F. and A.F. Clinical care of participants: M.M., M.N.R. and A.M.M. Created figures: H.S., D.B., N.P., R.A.M., K.E., J.B. and S.B.-R. Supervision: K.E., T.L., S.C.G. and A.F. Project administration: P.A. and M.W. Funding acquisition: S.C.G. Writing—original draft preparation: K.E., T.L., H.S., R.I.M., S.C.G., J.B. and S.B.-R. Review and editing of the paper: all authors.

Competing interests

Oxford University has entered into a partnership with AstraZeneca for further development of ChAdOx1 nCOv-19. S.C.G. is co-founder of Vaccitech (collaborators in the early development of this vaccine candidate) and named as an inventor on a patent covering the use of ChAdOx1-vectored vaccines and a patent application covering this SARS-CoV-2 vaccine. T.L. is named as an inventor on a patent application covering this SARS-CoV-2 vaccine and was a consultant to Vaccitech for an unrelated project. P.M.F. is a consultant to Vaccitech. A.J.P. is Chair of the UK Deptartment of Health and Social Care's (DHSC) Joint Committee on Vaccination & Immunisation (JCVI) but does not participate in discussions on COVID-19 vaccines and is a member of the World Health Organization's (WHO) Strategic Advisory Group of Experts. A.J.P. is an NIHR Senior Investigator. The views expressed in this article do not necessarily represent the views of DHSC, JCVI, NIHR or WHO. A.V.S.H. reports personal fees from Vaccitech outside of the submitted work and has a patent for ChAdOx1 licensed to Vaccitech and might benefit from royalty income to the University of Oxford from sales of this vaccine by AstraZeneca and sublicensees. M.S. reports grants from NIHR and non-financial support from AstraZeneca during the conduct of the study; grants from Janssen; grants from GlaxoSmithKline; grants from Medimmune; grants from Novavax; grants and non-financial support from Pfizer; and grants from MCM outside of the submitted work. C.G. reports personal fees from the Duke Human Vaccine Institute outside of the submitted work. A.D.D. reports grants and personal fees from AstraZeneca outside of the submitted work. In addition, A.D.D. has a patent for the manufacturing process of ChAdOx vectors with royalties paid to AstraZeneca and a patent for ChAdOx2 vector with royalties paid to AstraZeneca. The other authors declare no competing interests.

Additional information

Supplementary information is available for this paper at https://doi.org/10.1038/s41591-020-01194-5.

Correspondence and requests for materials should be addressed to K.J.E. or T.L.

Peer review information Alison Farrell is the primary editor on this article and managed its editorial process and peer review in collaboration with the rest of the editorial team.

Reprints and permissions information is available at www.nature.com/reprints.

nature research

Corresponding author(s): Katie Ewer and Teresa Lambe

Last updated by author(s): Nov 10, 2020

Reporting Summary

Nature Research wishes to improve the reproducibility of the work that we publish. This form provides structure for consistency and transparency in reporting. For further information on Nature Research policies, see our Editorial Policies and the Editorial Policy Checklist.

Statistics

For all statistical analyses, confirm that the following items are present in the figure legend, table legend, main text, or Methods section.

n/a	Confirmed
☐	☒ The exact sample size (*n*) for each experimental group/condition, given as a discrete number and unit of measurement
☐	☒ A statement on whether measurements were taken from distinct samples or whether the same sample was measured repeatedly
☐	☒ The statistical test(s) used AND whether they are one- or two-sided *Only common tests should be described solely by name; describe more complex techniques in the Methods section.*
☒	☐ A description of all covariates tested
☐	☒ A description of any assumptions or corrections, such as tests of normality and adjustment for multiple comparisons
☐	☒ A full description of the statistical parameters including central tendency (e.g. means) or other basic estimates (e.g. regression coefficient) AND variation (e.g. standard deviation) or associated estimates of uncertainty (e.g. confidence intervals)
☐	☒ For null hypothesis testing, the test statistic (e.g. *F*, *t*, *r*) with confidence intervals, effect sizes, degrees of freedom and *P* value noted *Give P values as exact values whenever suitable.*
☒	☐ For Bayesian analysis, information on the choice of priors and Markov chain Monte Carlo settings
☒	☐ For hierarchical and complex designs, identification of the appropriate level for tests and full reporting of outcomes
☒	☐ Estimates of effect sizes (e.g. Cohen's *d*, Pearson's *r*), indicating how they were calculated

Our web collection on statistics for biologists contains articles on many of the points above.

Software and code

Policy information about availability of computer code

Data collection	MESO QuickPlex SQ 120 (MSD), FACSDiva v8.02 (BD Biosciences), BioTek Gen5 v3.09, REDCap version 9.5.22; Vanderbilt University, Nashville, TN, USA
Data analysis	DISCOVERY WORKBENCH 4.0 (MSD), GraphPad Prism V8.4.3, IBM SPSS Statistics, BioTek Gen5 v3.09, SpectroFLo v2.2 (Cytek Biosciences) FlowJo v10.6.2 (BD BioSciences)

For manuscripts utilizing custom algorithms or software that are central to the research but not yet described in published literature, software must be made available to editors and reviewers. We strongly encourage code deposition in a community repository (e.g. GitHub). See the Nature Research guidelines for submitting code & software for further information.

Data

Policy information about availability of data

All manuscripts must include a data availability statement. This statement should provide the following information, where applicable:

- Accession codes, unique identifiers, or web links for publicly available datasets
- A list of figures that have associated raw data
- A description of any restrictions on data availability

Individual participant data will be made available when the trial is complete, upon requests directed to the corresponding author; after approval of a proposal, data can be shared through a secure online platform.

Field-specific reporting

Please select the one below that is the best fit for your research. If you are not sure, read the appropriate sections before making your selection.

☒ Life sciences ☐ Behavioural & social sciences ☐ Ecological, evolutionary & environmental sciences

For a reference copy of the document with all sections, see nature.com/documents/nr-reporting-summary-flat.pdf

Life sciences study design

All studies must disclose on these points even when the disclosure is negative.

Sample size	Power and sample size calculations were done for the primary efficacy only, which is not presented here. No specific power calculations were carried out for these immunogenicity subgroups which are secondary endpoints in the study and mostly descriptive in nature. The results presented in this manuscript are from an interim analysis of secondary or exploratory outcomes for the described groups of this phase I/II randomised control trial (NCT04324606). The primary efficacy analysis power calculation is described in the attached study protocol.
Data exclusions	All available data from eligible volunteers was included in the manuscript, with the exception of any individual data points which failed QC criteria described in the 'Replication' section below.
Replication	Aurora cytometry for tSNE analysis – Single technical replicates for each biological sample were ran. Experiments were ran on frozen PBMC samples so repeats were not possible. Instead, quality control criteria were applied to all samples, and samples that failed were excluded from analysis. QC criteria included: exclusion of any samples with a viable lymphocyte event count of <100,000 cells. All FACS plots were manually inspected to confirm quality of staining and cytometric acquisition. To maintain reproducibility between sample batches, the same cytometer was used for every run, the same lot of antibodies were used for all samples and gating and analysis was performed by a single operator. Aurora Intracellular cytokine staining - Single technical replicates for each biological sample were ran. Experiments were ran on frozen PBMC samples so repeats were not possible. Instead, quality control criteria were applied to all samples, and samples that failed were excluded from analysis. QC criteria included: exclusion of any samples with a viable CD4+ event count of <20,000 cells and any sample with <1% of cells being positive in the SEB sample for either IFNg, TNFa or IL2. All FACS plots were manually inspected to confirm quality of staining and cytometric acquisition. To maintain reproducibility between sample batches, the same cytometer was used for every run, the same lot of antibodies were used for all samples and gating and analysis was performed by a single operator. MSD - test samples were plated out in duplicate. Data was analysed using MSD discovery workbench 4.0. Samples were repeated if any sample a replicate with a coefficient of variations (CV) greater than 20%. Replicates were read off the standard curve, multiplied by dilution factor, and concentration was reported as an average of the replicates in pg/ml. Concentration from stimulated sample was subtracted from concentration from unstimulated (background subtract). Negative values of background subtract have been replaced by zeros. An arbitrary value of 0.0001 has been added to the background subtracts across all the samples to overcome the presence of null values raised from samples too low to be read off the standard curve. For the isotype and subclass standardised ELISAs (IgA, IgM, IgG1, and IgG3), test samples were plated in technical triplicates and a standard curve was included on every microplate, as well as 3 independent dilutions (internal controls) of the same standard curve serum diluted to correspond to the fourth dilution of the standard curve and plated in duplicate. Using Gen5 ELISA software v3.04 (BioTek), the standard curve OD values at 405 nm were fitted to a four-parameter model. Quality control was then performed on this curve as follows: the R2 value for the standard curve must be >0.994, the average interpolated AU of the internal control must be within 20% of the target value (equal in value to the dilution factor the internal control was plated at), the average OD at 405 nm of the blank control wells must be <0.15 OD405. Failure to meet these parameters results in the rejection of the experiment data, and the plate will be repeated. This ensures that the curve, interpolations and background of the assay are the same for every plate, and ensures that test samples are interpolated similarly between experiments. In addition, test samples must have a coefficient of variance in their OD405 values of <20%. Failure to meet this parameter results in the rejection of the data for that sample and the sample will be repeated. For the OD ELISAs (IgG2, IgG4 and IgE) samples were plated in technical duplicate. For the avidity ELISAs, samples were plated in technical duplicate. In addition, a standard serum pool was inlcuded on every plate and the IC50 calculated, data from any plates where the IC50 of the standard deviated >20% from the target value were discarded. Data for any samples for which the OD at 0M NaSCN across two replicates deviated by more than 20% was also discarded. ELISpot - plates were counted using an AID automated ELISpot counter (AID Diagnostika GmbH, algorithm C), using identical settings for all plates and spot counts were adjusted only to remove artefacts. Responses were averaged across triplicate wells and the mean response of the unstimulated (negative control) wells were subtracted. Results are expressed as spot forming cells (SFC)/106 PBMCs. Assays were ran on fresh cells only, therefore samples could not be repeated. Instead, QC criteria were applied to samples before inclusion in analysis. Responses to a peptide were considered positive if background subtracted responses were >40 SFU/106 PBMCs. If responses were >80 SFC/106 PBMC in the negative control (PBMC without antigen) or <800 SFC/106 PBMC in the positive control wells (pooled Staphylococcal enterotoxin B at 0.02 µg/mL and phytohaemagglutinin-L at 10 µg/mL), results were excluded from further analysis. Intracellular cytokine staining (Standard) – Single technical replicates for each biological sample were ran. Experiments were ran on freshly isolated samples so repeats were not possible. Instead, quality control criteria were applied to all samples, and samples that failed were excluded from analysis. QC criteria included: exclusion of any samples with a viable CD3+ event count of <100,000 cells and any sample with <1% of cells being positive in the SEB sample for either IFNg, TNFa or IL2. All FACS plots were manually inspected to confirm quality of staining and cytometric acquisition. To maintain reproducibility between sample batches, the same cytometer was used for every run, the same lot of antibodies were used for all samples and gating and analysis was performed by a single operator.
Randomization	Volunteers were randomized 1:1 to receive ChAdOx1 nCoV-19, except for a subset of 10 individuals who were not initially randomized, as detailed in the main study protocol which has been previously published.

Blinding	The study is single blinded (participant blinded). Investigators working on sample processing in the lab were blinded to group allocation. Investigators performing data collection and analysis were blinded to volunteer vaccination status.

Reporting for specific materials, systems and methods

We require information from authors about some types of materials, experimental systems and methods used in many studies. Here, indicate whether each material, system or method listed is relevant to your study. If you are not sure if a list item applies to your research, read the appropriate section before selecting a response.

Materials & experimental systems

n/a	Involved in the study
☐	☒ Antibodies
☐	☒ Eukaryotic cell lines
☒	☐ Palaeontology and archaeology
☒	☐ Animals and other organisms
☐	☒ Human research participants
☐	☒ Clinical data
☒	☐ Dual use research of concern

Methods

n/a	Involved in the study
☒	☐ ChIP-seq
☐	☒ Flow cytometry
☒	☐ MRI-based neuroimaging

Antibodies

Antibodies used

ELISPOT
Anti-human IFN-γ Monoclonal antibody, MABTECH, 3420-25A, 1-DIK, Lot 102, 1:100
Anti-IFN-γ Biotinylated monoclonal antibody, MABTECH, 3420-25A, 7-B6-1, Lot 102, 1:1000
Streptavidin-Alkaline Phosphatase, MABTECH, 3420-25A, Lot 102, 1:1000

MSD multiplex cytokine panel
Anti human IFN-γ antibody (50x) SulfoTag, MSD, K15010B-4, Clone: D21Q0-3, lot: D0081379, 1:50 dilution
Anti human IL-1β antibody (50x) SulfoTag, MSD, K15010B-4, Clone: D21AG-3, lot: D0081380, 1:50 dilution
Anti human IL-2 antibody (50x) SulfoTag, MSD, K15010B-4, Clone: D21QQ-3, lot: D0081320, 1:50 dilution
Anti human IL-4 antibody (50x) SulfoTag, MSD, K15010B-4, Clone: D21QR-3, lot: D0081302, 1:50 dilution
Anti human IL-8 antibody (50x) SulfoTag, MSD, K15010B-4, Clone: D21AN-3, lot: D0081255, 1:50 dilution
Anti human IL-10 antibody (50x) SulfoTag,MSD, K15010B-4, Clone: D21QU-3, lot: D0081343, 1:50 dilution
Anti human IL-12p70 antibody (50x) SulfoTag, MSD, K15010B-4, Clone: D21QV-3, lot: D0081307, 1:50 dilution
Anti human IL-13 antibody (50x) SulfoTag, MSD, K15010B-4, Clone: D21OD-3, lot: D0081381, 1:50 dilution
Anti human TNF-α antibody (50x) SulfoTag, MSD, K15010B-4, Clone: D21BH-3, lot: D0081382, 1:50 dilution

Flow Cytometry (Aurora and standard ICS):

Live/Dead Zombie UV, BioLegend, 423107, 1:250 dilution, lot 2176884
CD4 AF700, OKT4, BioLegend, 317425, 1:400 dilution lot B247388
CD19 Spark NIR 685, V CD19.11 BioLegend, 302269, 1:200 dilution, lot B311830
CD56 APC, 5.1H11, BioLegend, 362503, 1:100 dilution, lot B280822
CCR7 PER-CP/Cy5.5, G043H7 BioLegend, 353219, 1:50 dilution, lot B286436
PD1 PE/Dazzle 594, EH12.2H7, BioLegend, 329940, 1:100 dilution, lot B285543
CD57- PE/Cy7, HNK-1 BioLegend, 359624, 1:200 dilution, lot B277980
Interferon gamma BV650, 4S.B3, BioLegend, 502537, 1:100 dilution, lot B291938
IL2 BV605, MQ1-17H12, BioLegend, 500331, 1:100 dilution, lot B284324
CD107a BV785 H4A3, BioLegend, 328644 1:100 dilution, lot B284309
CD8 AF405, 3B5, ThermoFisher Scientific, MHCD0826, 1:100 dilution, lot 2201611
CD45RA SuperBright 702, HI100, ThermoFisher Scientific, 67-0458-41, 1:100 dilution, lot 2124807
CD27 PerCP eF710, O323,ThermoFisher Scientific, 46-0279-41, 1:100 dilution, lot 2129920
CD20 AF532, 2H7, ThermoFisher Scientific, 58-0209-42, 1:50 dilution, lot 2247567
Ki-67 APC eF780, SolA15, ThermoFisher Scientific, 47-5698-80, 1:100 dilution, lot 2162717
CD16 BUV496 BD BioSciences, 3G8, 564654, 1:200 dilution, lot 0051270
CD3 BUV661, OKT3, BD BioSciences 48-0037-41, 1:800 dilution, lot 0157849
CD138 BUV805, MI15, BD BioSciences, 748350, 1:100 dilution, lot 0156566
NKG2A BV480, 131411, BD BioSciences, 747923, 1:50 dilution, lot 0154607
IgM BB515, G20-127, BD BioSciences, 564622, 1:100 dilution, lot 9318220
IgG BV421, G18-145, BD BioSciences, 562581, 1:100 dilution, lot 9259706
TNF alpha BUV395, mAb11, BD BioSciences, 563996, 1:100 dilution, lot 0010280
CD69 BV750, FN50, BD BioSciences, 747522, 1:100 dilution, lot 0156563
CD71 BUV563, L01.1, BD BioSciences, 748314, 1:100 dilution, lot 0156565
CD25 BV737, M-A251, BD BioSciences, 356137, 1:800 dilution, lot 8218884
NKG2C PE, REA205, Miltenyi, 130-119-776, 1:200 dilution, lot 5200601467
KLRG1 VioBlue, 2F1/KLRG1, Miltenyi, 138421, 1:100 dilution, lot 5200704650
Anti-human CD28 Functional grade, eBioscience, 16-0289-85, 1:1000 dilution, lot 2197855
Anti-human CD49d Functional grade, eBioscience, 16-0499-85, 1:1000 dilution, lot 2062915
CD107a PE-Cy5, eBioH4A3, eBioscience, 15-1079-42, 1:1000 dilution, lot 2087212

CD8a APC-eF780, RPA-T8, eBioscience, 47-0088-42, 1:20 dilution, lot 2121889
Interferon gamma FITC, 4S.B3, eBioscience, 11-7319-82, 1:1000 dilution, lot 2204969
IL-2 BV650, MQ1-17H12, Biolegend, 500334, 1:100 dilution, lot B293289
IL-5 PE, JES1-39D10, Biolegend, 500904, 1:80 dilution, lot B60242
IL-13 APC, JES10-5A2, Biolegend, 501907, 1:40 dilution, lot B301070
TNF alpha PE-Cy7, MAb11, eBioscience, 25-7349-82, 1:4000 dilution, lot 2007278
CD3 AF700, UCHT1, eBioscience, 56-0038-82, 1:200 dilution, lot 2102327
CD4 PerCP Cy5.5, RPA-T4, eBioscience, 17-0049-42, 1:40 dilution, lot 1995457
CD14 eF450, 61D3, eBioscience, 48-0149-42, 1:400 dilution, lot 2146887
CD19 eF450, HIB19, eBioscience, 48-0199-42, 1:400 dilution, lot 2018427
CD45RA BV605, HI100, Biolegend, 304134, 1:4000 dilution, lot B254373
CCR7 BV711, G043H7, Bioscience, 353228, 1:100 dilution, B284686
LIVE/DEAD Fixable Aqua (405nm), Invitrogen, L34966, 1:1600 dilution, lot 2157201

ELISA:

Anti-Human IgG (γ-chain specific)–Alkaline Phosphatase antibody produced in goat, Sigma-Aldrich, A3187, Polyclonal, SLCG3196, 1:1000
Mouse Anti-Human IgG1 Hinge-AP, Southern Biotech, 9052-04, 4E3, G4015-MK18Z, 1:1000
Mouse Anti-Human IgG2 Fc-AP, Southern Biotech, 9060-04, 31-7-4, E2013-T035F, 1:500
Mouse Anti-Human IgG3 Hinge-AP, Southern Biotech, 9210-04, HP6050, F1818-TD48E, 1:500
Mouse Anti-Human IgG4 Fc-AP, Southern Biotech, 9200-04, HP6025, B3317-M788G, 1:1000
Goat Anti-Human IgA-AP, Southern Biotech, 2050-04, Polyclonal, C5213-R1660, 1:1000
Goat Anti-Human IgM-AP, Southern Biotech, 2020-04, Polyclonal, L4206-Q408D, 1:1000
Mouse Anti-Human IgE Fc-AP, Southern Biotech, 9160-04, B3102E8, J1617-X949D, 1:500
Recombinant Human IgG2 Lambda, Bio-Rad Laboratories Ltd, HCA108, AbD00264_hIgG2, 1607, 1:6400
Recombinant Human IgG4 Lambda, Bio-Rad Laboratories Ltd, HCA050A, AbD00264_hIgG4, 151154, 1:8000
Recombinant Human IgE Lambda, Bio-Rad Laboratories Ltd, HCA171, AbD00264_hIgE, 1807, 1:16000

Validation

Flow Cytometry (Aurora and standard ICS):

Each primary antibody was titrated in-house as a single stain on frozen naive human PBMC to determine the optimal concentration for separation between positive and negative cell populations. The full panel of antibodies were then tested together at working concentrations to confirm the quality of staining is similar when compensation is applied.
The Aurora antibodies: Live/Dead Zombie UV, BioLegend, 423107, lot 2176884. Zombie UV™ is an amine reactive fluorescent dye that is non-permeant to live cells, but permeant to the cells with compromised membranes. For flow cytometry, the suggested dilution is 1:100-1:1000 for 1-10 million cells.
Source (https://www.biolegend.com/en-us/products/zombie-uv-fixable-viability-kit-9336)

CD4 AF700, OKT4, BioLegend, 317425, 1:400 dilution lot B247388. CD4, also known as T4, is a 55 kD single-chain type I transmembrane glycoprotein expressed on most thymocytes, a subset of T cells, and monocytes/macrophages. The OKT4 antibody binds to the D3 domain of CD4. This antibody is routinely tested by flow cytometric analysis. Source (https://www.biolegend.com/en-us/search-results/alexa-fluor-700-anti-human-cd4-antibody-3661)

CD19 Spark NIR 685, V CD19.11 BioLegend, 302269, 1:200 dilution, lot B311830. CD19 is a 95 kD type I transmembrane glycoprotein also known as B4. It is a member of the immunoglobulin superfamily expressed on B-cells. Each lot of this antibody is quality control tested by immunofluorescent staining with flow cytometric analysis. For flow cytometric staining, the suggested use of this reagent is 5 µL per million cells in 100 µL staining volume
Cells. This antibody is routinely tested by flow cytometric analysis. Source (https://www.biolegend.com/en-us/products/spark-nir-685-anti-human-cd19-antibody-18623)

CD56 APC, 5.1H11, BioLegend, 362503, 1:100 dilution, lot B280822. CD56 is a single transmembrane glycoprotein also known as NCAM (neural cell adhesion molecule), Leu-19, or NKH1. It is a member of the Ig superfamily. The 140 kD isoform is expressed on NK and NKT cells. This antibody is routinely tested by flow cytometric analysis. Source (https://www.biolegend.com/en-gb/products/apc-anti-human-cd56-ncam-antibody-14587).

CCR7 PER-CP/Cy5.5, G043H7 BioLegend, 353219, 1:50 dilution, lot B286436. CCR7, also known as CD197, is a chemokine receptor that binds CCL19 and CCL21. CCR7 and its ligands link innate and adaptive immunity by affecting interactions between T cells and dendritic cells and their downstream effect. Each lot of this antibody is quality control tested by immunofluorescent staining with flow cytometric analysis. For flow cytometric staining, the suggested use of this reagent is 5 µl per million cells in 100 µl staining volume. This antibody is routinely tested by flow cytometric analysis. Source (https://www.biolegend.com/en-us/products/percp-cyanine5-5-anti-human-cd197-ccr7-antibody-7539)

PD1 PE/Dazzle 594, EH12.2H7, BioLegend, 329940, 1:100 dilution, lot B285543. Programmed cell death 1 (PD-1), also known as CD279, is a 55 kD member of the immunoglobulin superfamily. CD279 contains the immunoreceptor tyrosine-based inhibitory motif (ITIM) in the cytoplasmic region and plays a key role in peripheral tolerance and autoimmune disease. CD279 is expressed predominantly on activated T cells, B cells, and myeloid cells.
Each lot of this antibody is quality control tested by immunofluorescent staining with flow cytometric analysis. For flow cytometric staining, the suggested use of this reagent is 5 µl per million cells in 100 µl staining volume. This antibody is routinely tested by flow

cytometric analysis. Source (https://www.biolegend.com/en-us/search-results/pe-dazzle-594-anti-human-cd279-pd-1-antibody-9834).

CD57- PE/Cy7, HNK-1 BioLegend, 359624, 1:200 dilution, lot B277980. CD57, also known as HNK-1, NK-1, and Leu-7 is a 100-115 kD oligosaccharide antigenic determinant expressed on a variety of proteins, lipids, and chondroitin sulfate proteoglycans. CD57 is expressed on a subset of peripheral blood lymphocytes, including NK cells and CD8+ T cells. Each lot of this antibody is quality control tested by immunofluorescent staining with flow cytometric analysis. For flow cytometric staining, the suggested use of this reagent is 5 µl per million cells in 100 µl staining volume. This antibody is routinely tested by flow cytometric analysis. Source (https://www.biolegend.com/en-us/search-results/pe-cyanine7-anti-human-cd57-antibody-13715).

Interferon gamma BV650, 4S.B3, BioLegend, 502537, 1:100 dilution, lot B291938. Interferon-γ is a potent multifunctional cytokine which is secreted primarily by activated NK cells and T cells. Each lot of this antibody is quality control tested by intracellular immunofluorescent staining with flow cytometric analysis. For flow cytometric staining, the suggested use of this reagent is 5 µl per million cells in 100 µl staining volume. This antibody is routinely tested by flow cytometric analysis. Source (https://www.biolegend.com/en-us/search-results/brilliant-violet-650-anti-human-ifn-gamma-antibody-7678)

IL2 BV605, MQ1-17H12, BioLegend, 500331, 1:100 dilution, lot B284324. IL-2 is a potent lymphoid cell growth factor which exerts its biological activity primarily on T cells, promoting proliferation and maturation. Each lot of this antibody is quality control tested by immunofluorescent staining with flow cytometric analysis. For flow cytometric staining, the suggested use of this reagent is 5 µl per million cells in 100 µl staining volume. This antibody is routinely tested by flow cytometric analysis. Source (https://www.biolegend.com/en-us/products/brilliant-violet-605-anti-human-il-2-antibody-7676).

CD107a BV785 H4A3, BioLegend, 328644 1:100 dilution, lot B284309. CD107a, also known as Lysosome-Associated Membrane Protein 1 (LAMP-1) or LGP-120, is a 110-140 kD type I membrane glycoprotein. Mature CD107a is heavily glycosylated from a 40 kD core protein. This molecule is located on the luminal side of lysosomes. Upon activation, CD107a is transferred to the cell membrane surface of activated platelets, activated lymphocytes, macrophages, epithelial cells, endothelial cells, and some tumor cells. Each lot of this antibody is quality control tested by immunofluorescent staining with flow cytometric analysis. For flow cytometric staining, the suggested use of this reagent is 5 µl per million cells in 100 µl staining volume. This antibody is routinely tested by flow cytometric analysis. Source (https://www.biolegend.com/en-us/products/brilliant-violet-785-anti-human-cd107a-lamp-1-antibody-12095)

CD8 AF405, 3B5, ThermoFisher Scientific, MHCD0826, 1:100 dilution, lot 2201611. CD8 molecule is composed of two chains termed alpha and beta. CD8 is found on a T cell subset of normal cytotoxic / suppressor cells which make up approximately 20 to 35% of human peripheral blood lymphocytes. The CD8 antigen is also detected on natural killer cells, 80% of thymocytes, on a subpopulation of 30% of peripheral blood null cells and 15 to 30% of bone marrow cells. This antibody is routinely tested by flow cytometric analysis. Source (https://www.thermofisher.com/antibody/product/CD8-Antibody-clone-3B5-Monoclonal/MHCD0826).

CD45RA SuperBright 702, HI100, ThermoFisher Scientific, 67-0458-41, 1:100 dilution, lot 2124807. Description: The HI100 monoclonal antibody reacts with human CD45RA, a 220 kDa molecule expressed by subpopulations of CD4+ peripheral T lymphocytes, CD8+ peripheral T lymphocytes, and B cells. The CD45RA+ T cell populations are mainly naive/virgin allowing the use of HI100 mAb as a phenotypic marker to discriminate T cell subsets. This HI100 antibody has been pre-diluted and tested by flow cytometric analysis of normal human peripheral blood cells. This may be used at 5 µL (0.06 µg) per test This antibody is routinely tested by flow cytometric analysis. Source (https://www.thermofisher.com/antibody/product/CD45RA-Antibody-clone-HI100-Monoclonal/67-0458-42)

CD27 PerCP eF710, O323,ThermoFisher Scientific, 46-0279-41, 1:100 dilution, lot 2129920. The O323 monoclonal antibody reacts with human CD27, a lymphocyte-specific member of the TNFR superfamily. CD27 is expressed by a subset of thymocytes and virtually all mature T cells and is upregulated upon T-cell stimulation. CD27 binds to CD70, and through this interaction, plays an important role in T cell-B cell interaction. This O323 antibody has been pre-titrated and tested by flow cytometric analysis of normal human peripheral blood cells. This can be used at 5 µL (0.06 µg) per test. This antibody is routinely tested by flow cytometric analysis. Source (https://www.thermofisher.com/antibody/product/CD27-Antibody-clone-O323-Monoclonal/46-0279-42).

CD20 AF532, 2H7, ThermoFisher Scientific, 58-0209-42, 1:50 dilution, lot 2247567. The 2H7 monoclonal antibody reacts with human CD20, a 33-36 kDa transmembrane protein. CD20 is expressed by developing B cells as well as mature B cells but not plasma cells. CD20 has been detected at low levels on a small subset of mature T cells. It is suggested that CD20 plays a role in B-cell activation. This 2H7 antibody has been pre-diluted and tested by flow cytometric analysis of normal human peripheral blood cells. This may be used at 5 µL (0.06 µg) per test. This antibody is routinely tested by flow cytometric analysis. Source (https://www.thermofisher.com/antibody/product/CD20-Antibody-clone-2H7-Monoclonal/58-0209-42).

Ki-67 APC eF780, SolA15, ThermoFisher Scientific, 47-5698-80, 1:100 dilution, lot 2162717. The monoclonal antibody SolA15 recognizes mouse and rat Ki-67, a 300 kDa nuclear protein. Ki-67 is present during all active phases of the cell cycle (G1, S, G2, and mitosis), but is absent from resting cells (G0). Ki-67 is detected within the nucleus during interphase but redistributes to the chromosomes during mitosis. Ki-67 is used as a marker for determining the growth fraction of a given population of cells. This antibody can be used at less than or equal to 0.06 µg per test. Source (https://www.thermofisher.com/antibody/product/Ki-67-

Antibody-clone-SolA15-Monoclonal/47-5698-82).

CD16 BUV496 BD BioSciences, 3G8, 564654, 1:200 dilution, lot 0051270. The 3G8 monoclonal antibody specifically recognizes CD16a and CD16b, low affinity receptors for the Fc region of IgG. The recommended volume is 5µL/test. This antibody is routinely tested by flow cytometric analysis. Source (https://www.bdbiosciences.com/us/reagents/research/antibodies-buffers/immunology-reagents/anti-human-antibodies/cell-surface-antigens/buv496-mouse-anti-human-cd16-3g8/p/612944)

CD3 BUV661, OKT3, BD BioSciences 48-0037-41, 1:800 dilution, lot 0157849. he OKT3 monoclonal antibody specifically recognizes the CD3 epsilon subunit (CD3e/CD3ε) of the CD3 complex which consists of four transmembrane proteins (γ, δ, ε, ζ) that are associated with the T cell antigen receptor (TCR) to form the CD3/TCR complex. The CD3 complex associates with either TCR αβ or TCR γδ heterodimers that are alternatively expressed by some thymocytes, T cells or NKT cells. The CD3 complex is required for the cell surface expression and signal-transducing functions of the TCR. This antibody is routinely tested by flow cytometric analysis. Source (https://www.bdbiosciences.com/us/reagents/research/antibodies-buffers/immunology-reagents/anti-human-antibodies/cell-surface-antigens/buv661-mouse-anti-human-cd3-okt3/p/750972).

CD138 BUV805, MI15, BD BioSciences, 748350, 1:100 dilution, lot 0156566. The MI15 monoclonal antibody specifically binds to CD138 (Syndecan-1), an 85-92 kDa single chain transmembrane protein. It is also expressed on pre-B cells, immature B cells, and plasma cells, but not on mature circulating B-lymphocytes. This antibody was developed for use in flow cytometry. Source (https://www.bdbiosciences.com/eu/reagents/research/antibodies-buffers/immunology-reagents/anti-human-antibodies/cell-surface-antigens/buv805-mouse-anti-human-cd138-mi15/p/748350)

NKG2A BV480, 131411, BD BioSciences, 747923, 1:50 dilution, lot 0154607. The 131411 monoclonal antibody specifically recognizes NKG2A which is also known as NK cell receptor A, Natural killer cell lectin, Natural killer group protein 2, C-lectin type II protein, or CD159 antigen-like family member A (CD159a). NKG2A (CD159a) is encoded by KLRC1(killer cell lectin like receptor C1) which belongs to the killer cell lectin-like receptor (KLR) family. This antibody was developed for use in flow cytometry. Source (https://www.bdbiosciences.com/us/reagents/research/antibodies-buffers/immunology-reagents/anti-human-antibodies/cell-surface-antigens/bv480-mouse-anti-human-nkg2a-cd159a-131411/p/747923)

IgM BB515, G20-127, BD BioSciences, 564622, 1:100 dilution, lot 9318220. The G20-127 monoclonal antibody binds to the heavy chain of human IgM. The G20-127 antibody is not thought to react with other immunoglobulin heavy chain isotypes. This reagent has been pre-diluted for use at the recommended Volume per Test (5µL/test). This antibody is routinely tested by flow cytometric analysis. Source (https://www.bdbiosciences.com/us/applications/research/b-cell-research/immunoglobulins/human/bb515-mouse-anti-human-igm-g20-127/p/564622)

IgG BV421, G18-145, BD BioSciences, 562581, 1:100 dilution, lot 9259706. The G18-145 monoclonal antibody specifically binds to the heavy chain of human immunoglobulin G subclasses: IgG1, IgG2, IgG3 and IgG4. The G18-145 antibody has been reported not to react with the heavy chains of other human immunoglobulin isotypes. This reagent has been pre-diluted for use at the recommended Volume per Test (5µL/test). This antibody is routinely tested by flow cytometric analysis. Source (https://www.bdbiosciences.com/us/applications/research/b-cell-research/immunoglobulins/human/bv421-mouse-anti-human-igg-g18-145/p/562581)

TNF alpha BUV395, mAb11, BD BioSciences, 563996, 1:100 dilution, lot 0010280. The MAb11 monoclonal antibody specifically binds to human tumor necrosis factor (TNF, also known as TNF-α) protein. TNF is an efficient juxtacrine, paracrine and endocrine mediator of inflammatory and immune functions. This reagent has been pre-diluted for use at the recommended Volume per Test (5µL/test). This antibody is routinely tested by flow cytometric analysis. Source (https://www.bdbiosciences.com/us/applications/research/t-cell-immunology/th-1-cells/intracellular-markers/cytokines-and-chemokines/human/buv395-mouse-anti-human-tnf-mab11/p/563996).

CD69 BV750, FN50, BD BioSciences, 747522, 1:100 dilution, lot 0156563. The FN50 monoclonal antibody specifically binds to human CD69. CD69 is also known as activation-induced molecule (AIM), early activation antigen (EA-1), very early activation antigen (VEA), C-type lectin domain family 2 member C (CLEC2C), MLR-3, GP32/28 and Leu-23. CD69 is a transmembrane type II homodimer receptor. CD69 is comprised of disulfide-linked, differentially glycosylated core protein subunits that are approximately 28 and 34 kDa in size. Each subunit contains a C-type lectin domain. CD69 is expressed on activated T, B, and natural killer (NK) lymphocytes, thymocytes, neutrophils, eosinophils and platelets. This antibody was developed for use in flow cytometry. This antibody is routinely tested by flow cytometric analysis. Source (https://www.bdbiosciences.com/us/reagents/research/antibodies-buffers/immunology-reagents/anti-human-antibodies/cell-surface-antigens/bv750-mouse-anti-human-cd69-fn50-also-known-as-fn-50/p/747522).

CD71 BUV563, L01.1, BD BioSciences, 748314, 1:100 dilution, lot 0156565. The L01.1 monoclonal antibody specifically binds to CD71 which is also known as the transferrin receptor (TFR). This type II transmembrane glycoprotein is expressed on cells as a disulfide-linked homodimer comprised of 95 kDa monomers. CD71 is expressed on activated lymphocytes, monocytes, macrophages, brain endothelium, and most proliferating cells. This antibody was developed for use in flow cytometry. This antibody is routinely tested by flow cytometric analysis. Source (https://www.bdbiosciences.com/eu/reagents/research/antibodies-buffers/immunology-reagents/anti-human-antibodies/cell-surface-antigens/buv563-mouse-anti-human-cd71-l011/p/748314).

CD25 BV737, M-A251, BD BioSciences, 356137, 1:800 dilution, lot 8218884 The M-A251 monoclonal antibody specifically binds to the 55 kDa type I transmembrane glycoprotein known as low-affinity interleukin-2 receptor alpha chain subunit (IL-2Rα). CD25 is expressed on regulatory T cells, activated lymphocytes (T and B), and monocytes. This antibody was developed for use in flow cytometry. This antibody is routinely tested by flow cytometric analysis. Source (https://www.bdbiosciences.com/us/reagents/research/antibodies-buffers/immunology-reagents/anti-human-antibodies/cell-surface-antigens/buv737-mouse-anti-human-cd25-m-a251/p/741832).

NKG2C PE, REA205, Miltenyi, 130-119-776, 1:200 dilution, lot 5200601467. Clone REA205 recognizes the CD159c antigen, a calcium-dependent (C-type) lectin which is also known as NKG2C type II integral membrane protein or KLRC2. This antibody is recommended at a dilution of 1:50. Source (https://www.miltenyibiotec.com/GB-en/products/cd159c-nkg2c-antibody-anti-human-reafinity-rea205.html#gref)

KLRG1 VioBlue, 2F1/KLRG1, Miltenyi, 138421, 1:100 dilution, lot 5200704650. Clone REA261 recognizes the killer cell lectin-like receptor subfamily G member 1 (KLRG1) antigen, a transmembrane protein, which is also known as C-type lectin domain family 15 member A (CLEC15A) or ITIM-containing receptor MAFA-L. KLRG1 is expressed by basophils, CD4 and CD8 T cells that exhibit a memory cell phenotype, and by a large proportion of peripheral blood NK cells. This antibody is recommended at a dilution of 1:50. Source (https://www.miltenyibiotec.com/GB-en/products/klrg1-antibody-anti-human-reafinity-rea261.html#gref).

Anti-human CD28 Functional grade, eBioscience, 16-0289-85, 1:1000 dilution, lot 2197855. The CD28.6 monoclonal antibody reacts with the human CD28 molecule, a 44 kDa homodimer expressed by thymocytes, mature T cells and plasma cells. This antibody is used frequently for functional T cell stimulation. Source (https://www.thermofisher.com/antibody/product/CD28-Antibody-clone-CD28-6-Monoclonal/16-0288-81)

Anti-human CD49d Functional grade, eBioscience, 16-0499-85, 1:1000 dilution, lot 2062915. The 9F10 monoclonal antibody reacts with human CD49d, the 150 kDa integrin alpha4 subunit. The complex of CD49d non-covalently associated with integrin beta1 (CD29), also known as VLA-4, is a receptor for fibronectin and VCAM-1 (CD106). This complex is expressed by thymocytes, peripheral lymphocytes, monocytes and eosinophils. This antibody is used frequently for functional T cell stimulation. Source (https://www.thermofisher.com/antibody/product/CD49d-Integrin-alpha-4-Antibody-clone-9F10-Monoclonal/16-0499-81).

CD107a PE-Cy5, eBioH4A3, eBioscience, 15-1079-42, 1:1000 dilution, lot 2087212
Description: The eBioH4A3 monoclonal antibody reacts with human CD107a, also known as lysosomal-associated membrane protein-1 (LAMP-1). CD107a is a highly glycosylated protein of approximately 110kDa. It is predominantly expressed intracellularly in the lysosomal/endosomal membrane in nearly all cells. CD107a is transiently expressed on the cell surface of degranulating cytolytic T cells, and is also upregulated on the surface of activated platelets and some cancer cells.
his eBioH4A3 antibody has been reported for use in intracellular staining followed by flow cytometric analysis. It has also been reported for use in surface staining in a flow cytometric based degranulation assay.
Source: https://www.thermofisher.com/antibody/product/CD107a-LAMP-1-Antibody-clone-eBioH4A3-Monoclonal/15-1079-42

CD8a APC-eF780, RPA-T8, eBioscience, 47-0088-42, 1:20 dilution, lot 2121889
The RPA-T8 monoclonal antibody reacts with the human CD8a molecule, an approximately 32-34 kDa cell surface receptor expressed either as a heterodimer with the CD8 beta chain (CD8 alpha/beta) or as a homodimer (CD8 alpha/alpha). A majority of thymocytes and a subpopulation of mature T cells and NK cells express CD8a. CD8 binds to MHC class I and through its association with protein tyrosine kinase p56lck plays a role in T-cell development and activation of mature T cells.
This RPA-T8 antibody has been reported for use in flow cytometric analysis.
Source: https://www.thermofisher.com/antibody/product/CD8a-Antibody-clone-RPA-T8-Monoclonal/47-0088-42

Interferon gamma FITC, 4S.B3, eBioscience, 11-7319-82, 1:1000 dilution, lot 2204969
The 4S.B3 monoclonal antibody reacts with interferon-gamma (IFN gamma). Human IFN gamma is a 17 kDa factor produced by activated T and NK cells and is an anti-viral and anti-parasitic cytokine. IFN gamma in synergy with other cytokines, such as TNF alpha, inhibits proliferation of normal and transformed cells. Immunomodulatory effects of IFN gamma are exerted on a wide range of cell types expressing the high affinity receptors for IFN gamma. Glycosylation of IFN gamma does not affect its biological activity.
The 4S.B3 antibody has been reported for use in intracellular staining for flow cytometric analysis.
Source: https://www.thermofisher.com/antibody/product/IFN-gamma-Antibody-clone-4S-B3-Monoclonal/11-7319-82

IL-2 BV650, MQ1-17H12, Biolegend, 500334, 1:100 dilution, lot B293289
IL-2 is a potent lymphoid cell growth factor which exerts its biological activity primarily on T cells, promoting proliferation and maturation. Additionally, IL-2 has been found to stimulate growth and differentiation of B cells, NK cells, LAK cells, monocytes, and oligodendrocytes.
Each lot of this antibody is quality control tested by intracellular immunofluorescent staining with flow cytometric analysis.
Source (https://www.biolegend.com/en-us/products/brilliant-violet-650-anti-human-il-2-antibody-7768)

IL-5 PE, JES1-39D10, Biolegend, 500904, 1:80 dilution, lot B60242
L-5 is a homodimeric, disulphide-linked protein produced by T-cells. Monomeric human IL-5 is a 126 amino acid protein with a reported molecular weight of 26 kD for the homodimeric protein. Mouse and human IL-5 are approximately 70% identical. IL-5 has been shown to promote the growth of immature hematopoietic BFU-E progenitors, stimulate the activation and differentiation of eosinophils, and promote the generation of cytotoxic lymphocytes. The JES1-39D10 antibody can neutralize the bioactivity of natural or recombinant IL-5.
Each lot of this antibody is quality control tested by intracellular immunofluorescent staining with flow cytometric analysis.
Source (https://www.biolegend.com/en-us/products/pe-anti-human-il-5-antibody-934)

IL-13 APC, JES10-5A2, Biolegend, 501907, 1:40 dilution, lot B301070

IL-13 is an immunoregulatory cytokine produced primarily by activated Th2 lymphocytes. IL-13 shares 30% amino acid sequence homology with IL-4 and demonstrates similar biological activities. The biological activities of IL-13 include: suppression of macrophage cytotoxic activity, upregulation of IL-1RA expression, and suppression of proinflammatory cytokine secretion. The JES10-5A2 antibody reacts with human interleukin-13 (IL-13). The JES10-5A2 antibody can neutralize the bioactivity of natural or recombinant IL-13.
Each lot of this antibody is quality control tested by intracellular immunofluorescent staining with flow cytometric analysis.
Source https://www.biolegend.com/en-us/products/apc-anti-human-il-13-antibody-938

TNF alpha PE-Cy7, MAb11, eBioscience, 25-7349-82, 1:4000 dilution, lot 2007278
The MAb11 antibody reacts with human tumor necrosis factor-alpha (TNF alpha), a 17 kDa cytokine produced by monocytes, macrophages, neutrophils, NK cells and CD4+ T cells. TN alpha has cytolytic activity against a range of tumor cells and is important in immune regulation. TNF alpha forms dimers and trimers and also exists as a 26 kDa membrane bound form. The MAb11 antibody is a neutralizing antibody.
This MAb11 antibody has been reported for use in intracellular staining followed by flow cytometric analysis.
Source https://www.biolegend.com/en-us/products-2/alexa-fluor-488-anti-human-tnf-alpha-antibody-2750

CD3 AF700, UCHT1, eBioscience, 56-0038-82, 1:200 dilution, lot 2102327
CD3ε is a 20 kD chain of the CD3/T-cell receptor (TCR) complex which is composed of two CD3ε, one CD3γ, one CD3δ, one CD3ζ (CD247), and a T-cell receptor (α/β or γ/δ) heterodimer. It is found on all mature T lymphocytes, NK-T cells, and some thymocytes. CD3, also known as T3, is a member of the immunoglobulin superfamily that plays a role in antigen recognition, signal transduction, and T cell activation.
Each lot of this antibody is quality control tested by immunofluorescent staining with flow cytometric analysis.
Source: https://www.biolegend.com/en-us/products/alexa-fluor-700-anti-human-cd3-antibody-3417

CD4 PerCP Cy5.5, RPA-T4, eBioscience, 17-0049-42, 1:40 dilution, lot 1995457
CD4, also known as T4, is a 55 kD single-chain type I transmembrane glycoprotein expressed on most thymocytes, a subset of T cells, and monocytes/macrophages. CD4, a member of the Ig superfamily, recognizes antigens associated with MHC class II molecules, and participates in cell-cell interactions, thymic differentiation, and signal transduction. CD4 acts as a primary receptor for HIV, binding to HIV gp120. CD4 has also been shown to interact with IL-16.
Each lot of this antibody is quality control tested by immunofluorescent staining with flow cytometric analysis.
Source: https://www.biolegend.com/en-us/products/alexa-fluor-488-anti-human-cd4-antibody-2727

CD14 eF450, 61D3, eBioscience, 48-0149-42, 1:400 dilution, lot 2146887
The 61D3 monoclonal antibody reacts with human CD14, a 53-55 kDa GPI-linked glycoprotein. CD14 is expressed on monocytes, interfollicular macrophages and some dendritic cells. Complexes of LPS and LBP (LPS-Binding Protein) bind with high affinity to monocytes through the surface CD14.
This antibody is routinely tested by flow cytometric analysis.
Source: https://www.thermofisher.com/antibody/product/CD14-Antibody-clone-61D3-Monoclonal/48-0149-42

CD19 eF450, HIB19, eBioscience, 48-0199-42, 1:400 dilution, lot 2018427
he HIB19 monoclonal antibody reacts with human CD19, a 95 kDa transmembrane glycoprotein. CD19 is expressed by B cells during all stages of development excluding the terminally differentiated plasma cells. Follicular dendritic cells also express CD19. Together CD21, CD81, Leu13, MHC class II, and CD19 form a multimolecular complex that associates with BCR. Signaling through CD19 induces tyrosine phosphorylation, calcium flux and proliferation of B cells. The SJ25C1 antibody and the HIB19 monoclonal antibody recognize overlapping epitopes.
This HIB19 antibody has been reported for use in flow cytometric analysis.
Source https://www.thermofisher.com/antibody/product/CD19-Antibody-clone-HIB19-Monoclonal/25-0199-42

CD45RA BV605, HI100, Biolegend, 304134, 1:4000 dilution, lot B254373
The HI100 monoclonal antibody reacts with human CD45RA, a 220 kDa molecule expressed by subpopulations of CD4+ peripheral T lymphocytes, CD8+ peripheral T lymphocytes, and B cells. The CD45RA+ T cell populations are mainly naive/virgin allowing the use of HI100 mAb as a phenotypic marker to discriminate T cell subsets.
This HI100 antibody has been reported for use in flow cytometric analysis.
Source: https://www.thermofisher.com/antibody/product/CD45RA-Antibody-clone-HI100-Monoclonal/25-0458-42

CCR7 BV711, G043H7, Bioscience, 353228, 1:100 dilution, B284686
CCR7, also known as CD197, is a chemokine receptor that binds CCL19 and CCL21. CCR7 and its ligands link innate and adaptive immunity by affecting interactions between T cells and dendritic cells and their downstream effect. Naïve T cells enter the lymph node through high endothelial venules, which express CCL21. Dendritic cells and macrophages enter the lymph node through afferent lymphatics. The encounter of T cells and dendritic cells in the T cell zone is CCR7-dependent. In addition, during immunological surveillance, B cells recirculate between B-cell-rich compartments (follicles or B cell zones) in secondary lymphoid organs, surveying for antigen. After antigen binding, B cells move to the boundary of B and T zones to interact with T-helper cells; this B cell migration is directed by CCR7 and its ligands. CCR7-positive cancer cell expression has been associated with lymph node metastasis.
Each lot of this antibody is quality control tested by immunofluorescent staining with flow cytometric analysis.
Source https://www.biolegend.com/en-us/products/alexa-fluor-488-anti-human-cd197-ccr7-antibody-7496

LIVE/DEAD Fixable Aqua (405nm), Invitrogen, L34966, 1:1600 dilution, lot 2157201
The Live/Dead Cell Double Staining Kit is utilized for simultaneous fluorescence staining of viable and dead cells. This kit contains calcein-AM and propidium iodide (PI) solutions, which stain viable and dead cells, respectively. Calcein-AM, acetoxymethyl ester of calcein, is highly lipophilic and cell membrane permeable. Though calcein-AM itself is not a fluorescent molecule, the calcein generated from Calcein-AM by esterase in a viable cell emits a strong green fluorescence (λex 490 nm, λem 515 nm). Therefore, calcein-AM only stains viable cells.
Source: https://www.sigmaaldrich.com/catalog/product/sigma/04511?lang=en&region=GB

ELISA:

Anti-Human IgG (γ-chain specific)–Alkaline Phosphatase antibody produced in goat, Sigma-Aldrich, A3187, Polyclonal, SLCG3196. The A3187 antibody specifically binds to human IgG γ-chain. This antibody is routinely tested in ELISA (Source: https://www.sigmaaldrich.com/catalog/product/sigma/a3187?lang=en&region=GB)

Mouse Anti-Human IgG1 Hinge-AP, Southern Biotech, 9052-04, 4E3, G4015-MK18Z. The 9052-04 specifically binds to human IgG1 hinge region. This antibody is routinely tested in ELISA (Source: https://www.southernbiotech.com/?catno=9052-04&type=Monoclonal#&panel2-1)

Mouse Anti-Human IgG2 Fd-AP, Southern Biotech, 9080-04, 31-7-4, E2013-T035F. The 9080-04 specifically binds to human IgG2 Fd region. This antibody is routinely tested in ELISA (Source: https://www.southernbiotech.com/?catno=9080-04&type=Monoclonal#&panel2-1)

Mouse Anti-Human IgG3 Hinge-AP, Southern Biotech, 9210-04, HP6050, F1818-TD48E. The 9210-04 specifically binds to human IgG3 hinge region. This antibody is routinely tested in ELISA (Source: https://www.southernbiotech.com/?catno=9210-04&type=Monoclonal#&panel2-1)

Mouse Anti-Human IgG4 Fc-AP, Southern Biotech, 9200-04, HP6025, B3317-M788G. The 9200-04 specifically binds to human IgG4 Fc region. This antibody is routinely tested in ELISA (Source: https://www.southernbiotech.com/?catno=9200-04&type=Monoclonal#&panel2-1)

Goat Anti-Human IgA-AP, Southern Biotech, 2050-04, Polyclonal, C5213-R1660. The 2050-04 specifically binds to human IgA heavy chain. This antibody is routinely tested in ELISA (Source: https://www.southernbiotech.com/?catno=2050-04&type=Polyclonal#&panel2-1)

Goat Anti-Human IgM-AP, Southern Biotech, 2020-04, Polyclonal, L4206-Q408D. The 2020-04 specifically binds to human IgM heavy chain. This antibody is routinely tested in ELISA (Source: https://www.southernbiotech.com/?catno=2020-04&type=Polyclonal#&panel2-1)

Mouse Anti-Human IgE Fc-AP, Southern Biotech, 9160-04, B3102E8, J1617-X949D. The 9160-04 specifically binds to human IgE Fc region. This antibody is routinely tested in ELISA (Source: https://www.southernbiotech.com/?catno=9160-04&type=Monoclonal#&panel2-1)

Recombinant Human IgG2 Lambda, Bio-Rad Laboratories Ltd, HCA108, AbD00264_hIgG2, 1607. The HCA108 is a recombinant antibody that has no known reactivity with mammalian proteins or other antigens. This antibody is routinely tested in ELISA (Source: https://www.bio-rad-antibodies.com/protein/human-igg2-recombinant-protein-abd00264-higg2-hca108.html?f=purified)

Recombinant Human IgG4 Lambda, Bio-Rad Laboratories Ltd, HCA050A, AbD00264_hIgG4, 151154. The HCA050A is a recombinant antibody that has no known reactivity with mammalian proteins or other antigens. This antibody is routinely tested in ELISA (Source: https://www.bio-rad-antibodies.com/protein/human-igg4-recombinant-protein-abd00264-higg4-hca050.html?f=purified)

Recombinant Human IgE Lambda, Bio-Rad Laboratories Ltd, HCA171, AbD00264_hIgE, 1807. The HCA171 is a recombinant antibody that has no known reactivity with mammalian proteins or other antigens. This antibody is routinely tested in ELISA (Source: https://www.bio-rad-antibodies.com/protein/human-ige-recombinant-protein-abd00264-hige-hca171.html?f=purified)

ELISPOT

All antibody used in this assay were titrated in house.

Anti-human IFN-γ acts as a capture antibody that binds specifically to human IFN-γ
Anti-IFN-γ (biotinylated) acts as a detection antibody which specifically binds to IFNγ

Both antibodies are routinely used and tested across ELISpot IFNγ. Further information can be found https://www.mabtech.com/products/human-ifn-gamma-elispot-basic-kit-kit-alp_3420-2a#tabs-min-1

MSD multiplex cytokine panel

MSD offers V-PLEX assays for customers who require unsurpassed performance and quality. V-PLEX products are developed under rigorous design control and are fully validated according to fit-for-purpose39 principles in accordance with MSD's Quality Management System. They offer exceptional sensitivity, simple protocols, reproducible results, and lot-to-lot consistency. In addition

to the analytical validation, robustness of the assay protocol is assessed during development along with the stability and robustness of the assay components and kits. Specific details of their antibody validation is confidential. Further information can be found at https://www.mesoscale.com/en/products/human-th1-th2-10-plex-tissue-culture-kit-k15010b/

Eukaryotic cell lines

Policy information about cell lines

Cell line source(s)	Expi293™ (Thermo Fisher Scientific)
Authentication	None
Mycoplasma contamination	Cell lines were not tested for mycoplasma contamination.
Commonly misidentified lines (See ICLAC register)	None

Human research participants

Policy information about studies involving human research participants

Population characteristics	Male and Female healthy adult volunteers aged 18-55 years old were recruited from 5 sites across the UK
Recruitment	The results described are for a phase I/II trial in a healthy volunteer population with minimal co-morbidity. Recruitment was carried out through general advertisement including the study website and online social media adverts. Participants were pre-screened through an online questionnaire covering the main eligibility criteria. A formal in-person screening visit then took place and participants were enrolled if meeting the eligibility criteria. Participants without access to the internet were able to answer the pre-screening questions via phone. Individuals without access to the internet, phone communication and who were solely reliant on public transport were unable to take part. As a phase I/II healthy volunteer trial this is likely to have had minimal impact on the validity of the results. Further assessment of the vaccine in the target population will take place in phase III trials (not presented here) which will increase the generalisability of results.
Ethics oversight	This study was approved in the UK by the Medicines and Healthcare products Regulatory Agency (reference 21584/0424/001-0001) and the South Central Berkshire Research Ethics Committee (reference 20/SC/0145).

Note that full information on the approval of the study protocol must also be provided in the manuscript.

Clinical data

Policy information about clinical studies

All manuscripts should comply with the ICMJE guidelines for publication of clinical research and a completed CONSORT checklist must be included with all submissions.

Clinical trial registration	ISRCTN [15281137] and ClinicalTrials.gov [NCT04324606]
Study protocol	The trial protocol can be accessed as supplementary data in Folegatti PM and Ewer KJ et al., Safety and immunogenicity of the ChAdOx1 nCoV-19 vaccine against SARS-CoV-2: a preliminary report of a phase 1/2, single-blind, randomised controlled trial. Lancet. 2020 Aug 15;396(10249):467-478. doi: 10.1016/S0140-6736(20)31604-4. PMID: 32702298; PMCID: PMC7445431.
Data collection	Participants were recruited between April 23 and May 21, 2020 from 5 different sites across the UK (Centre for Clinical Vaccinology and Tropical Medicine, University of Oxford; NIHR Southampton Clinical Research Facility, University Hospital Southampton NHS Foundation Trust, Southampton; Clinical Research Facility, Imperial College London; St Georges University of London and University Hospital NHS Foundation Trust; and University Hospitals Bristol and Weston NHS Foundation Trust
Outcomes	This manuscript reports on secondary immunogenicity outcomes. Immunogenicity outcomes were assessed through tSNE analysis, multiplex cytokine analysis, ELISA, IFN-gamma ELISPOT, flow cytometry and intracellular cytokine staining.

Flow Cytometry

Plots

Confirm that:

☒ The axis labels state the marker and fluorochrome used (e.g. CD4-FITC).

☒ The axis scales are clearly visible. Include numbers along axes only for bottom left plot of group (a 'group' is an analysis of identical markers).

☒ All plots are contour plots with outliers or pseudocolor plots.

☒ A numerical value for number of cells or percentage (with statistics) is provided.

Methodology

Sample preparation	Aurora samples:

Sample preparation

The samples used for flow cytometry on the Cytek Aurora spectral analyser were frozen aliquots of peripheral blood mononuclear cells (PBMCs) of 30 donors from days 0, 7, 14 and 28 after vaccination with ChAdOx1 nCoV19 (n=26). Cells were defrosted in media containing >5U/mL benzonase and re-suspended in complete RPMI media supplemented with 10% FCS, L-glutamine and Penicillin/streptomycin at a concentration of 2x107cells/mL. 2x106 PBMCs per well were plated in a 96-well plate and stimulated with synthetic peptides spanning the SARS-CoV-2 Spike protein split into two separate pools for the S1 and S2 subunits (Supplementary table S2) at a final concentration of 2µg/mL, or media as a control. One well per donor was stimulated with Phorbol 12-myristate 13-acetate (PMA, BioLegend) as a positive control. PBMCs were co-stimulated in the presence of anti-human CD28, CD49d (1µg/mL, Life Technologies Ltd), and CD107a-BV786 (BioLegend) for two hours at 37°C with 5% CO2, and then incubated for a further 16 hours after the addition of 1µg/mL Brefeldin A and Monensin to each well (BioLegend).

Standard ICS samples:
Intracellular cytokine staining (ICS) was performed on freshly isolated PBMCs stimulated with pooled S1 and S2 peptides. 3 x 106 PBMCs were resuspended in 5 ml polypropylene FACS tubes to a volume of 1 ml in R10 media supplemented with 1 µg/ml anti-human CD28 and CD49d and 1 µl CD107a PE-Cy5 (eBioscience). S1 and S2 peptide pools (Supplementary table S2) were added at a concentration of 2 µg/ml. Each sample also included a positive control (Staphylococcal enterotoxin B at 1 µg/ml, Sigma Aldrich) and an unstimulated (media only) control. Cells were incubated at 37°C with 5% CO2 for 16-20 hours with Brefeldin A (3 µg/ml) and monensin (2mM) (eBioscience) added after 2 hours.

At the end of the incubation, cells were washed in FACS buffer (PBS containing 0.1% bovine serum albumin and 0.01% NaN3) and transferred to a 96 well U-bottom tissue culture plate for staining . A surface staining cocktail was first added containing 2.5 µl of a 1:40 dilution of Aqua Live/Dead stain (ThermoFisher Scientific) and 1 µl of BV711 CCR7 (Biolegend) in 46.5 µl FACS buffer. Cells were incubated in the dark for 20 minutes and washed with FACS buffer. 100 µl CytoFix/CytoPerm solution (BD Biosciences) was added to each well and left to incubate for a further 20 minutes. Cells were then washed with Perm/Wash buffer before intracellular cytokine staining. The ICS cocktail contained 0.025 µl CD45RA BV605, 0.025 µl TNFαa PE-Cy7, 0.1 µl IFNgy FITC, 0.025 µl CD14 e450, 0.025 µl CD19 e450, 0.5 µl CD3 AF700, 1 µl IL-2 BV650, 1.25 µl IL-5 PE, 2.5 µl IL-13 APC, 3.5 µl CD4 PerCP Cy5.5 and 5 µl CD8 APC-eF780 to a total volume of 50 µl diluted in FACS buffer. Samples were stained in the dark for 30 minutes. Cells were washed twice with perm/wash buffer and twice with FACS buffer before being resuspended in 100 µl of 1% paraformaldehyde.

Compensation controls were prepared fresh for each batch using OneComp eBeads (eBioscience). Cells were kept on ice and strained through a 35 µmm filter before acquisition. Cells were acquired on a 5-laser BD LSRFortessa flow cytometer (BD Biosciences) and data analysed in FlowJo v10.7. A hierarchical gating strategy was applied for sample analysis (Supplementary figure 7). A QC process was applied to remove samples with fewer than 100,000 events in the live CD3+ gate, samples with <1% cytokine response to SEB (CD4+ and CD8+ IFN□, CD8+ TNF□). A lower limit of detection was applied and only samples with an ELISPOT response greater than 200 SFC/106 PBMC were included in the analysis].

Instrument

Cytek Aurora, Custom build with 4 lasers (Cytek Biosciences) and LSRFortessa-X20, 5 laser (Becton Dickinson)

Software

SpectroFLo v2.2 (Cytek Biosciences)
FACSDiva v 8.02 (BD Biosciences)
FlowJo v10.6.2 (BD Biosciences)
Prism v8 (GraphPad)

Cell population abundance

For Aurora tSNE analysis, live single cell lymphocytes were the cell type of interest. The median event count across all samples analysed was 435000 [Range: 107274-741000, IQR: 271137-588000].

For Aurora Intracellular cytokine staining live single cell lymphocytes were the cell type of interest. The median event count across all samples analysed was 465500 [Range: 42886-923000, IQR: 254193-694250].

For standard intracellular cytokine staining experiments, the cell population of interest was single cell viable CD3+ lymphoyctes. The median event count across all samples analysed was 603000 [range: 163693-918000, IQR: 462250-703250].

Gating strategy

Cytek Aurora analysis:
1.Y=Live/Dead Zombie UV X=FSC-A. Live population gated
2. Y=FSC-H, X= FSC-A, Cells along the diagonal axis gated
3. Y= SSC-A, X= FSC-A, Lymphocytes gated and defined as the population of cells within the X=0.5M-2.0M and Y=0.3M-1.0M range.
4. Y=CD19 Spark NIR685 X= CD3 BUV661.

a) B cells defined as Y>-7*103, X=-102 – 3*103
b) CD3+ cells defined as Y=-9*103 - 1, X>6*103
c) CD19-CD3- cells defined as Y=-8*103 - 0, X=-102 - 3*103.

5. CD3+ T cells
a) CD8+ T cells defined as Y=2*104 – 2*105, X= -7*103 - 3*103
b) CD4+ T cells defined as Y= -104 - 104, X= 4*103 – 3*104.
Within each population of CD4 or CD8 T cells:
c) Y=CD45RA = 7*103 X=CCR7 = 3*103
d) Y=Ki67 Y>7*103 X=FSC-A
e) Y=CD57 = 2*104, X= CD57= 2*103
f) Y=CD69= 104, X= CD25 = 5*103

g) Y=IFN-gamma = diagonal from 3*104 - 104, X= CD107a = 105
h) Y=TNF-alpha = 2*103, X= IL2 = 9*103

6. CD19+ B cells
a) Y=IgG=9*103, X =CD27=3*103
b) Y=CD71= 104, X= Ki67= 6*104

7. CD19-CD3- cells
NK cells defined as Y=CD56= diagonal from 2*104 to 5*103 when X=6*104. Then Y=-2*103. X=CD16= >0.
Within NK cells
Y=CD57=2*103, X=NKG2C=3*103
Y=Ki67 => 5*104, X= CD56 => -3*103.

Standard ICS analysis:
(Parent lymphocyte gating)
1: X = FSC-A, Y=SSC-A, lymphocyte population gated
2: X = FSC-A, Y=FSC-H, single cell population gated
3: X = Live/Dead Aqua = 2x10^3(upper limit), Y = CD3 AF700 = 2x10^2
4: X = Dump(CD14-/CD19-) e450 = 1x10^3(upper limit), Y = SSC-H (all events)

(CD4+ T cell gating)
5: X = CD4 PerCP Cy5.5 = 7x10^2, Y = IFNγ FITC (all events)
6: X = CD8 APC-eF780 = 3x10^2(upper limit), Y = IFNγ FITC (all events)
6a: X = IFNγ FITC = 5x10^2, Y = IL-2 BV650 = 3x10^3
6b: X = IFNγ FITC (all events), Y = TNFα PE-Cy7 = 5x10^2
6c: X = IFNγ FITC (all events), Y = IL-5 PE = 1x10^3
6d: X = IFNγ FITC (all events), Y = IL-13 APC = 1x10^3

(CD8+ T cell gating)
7: X = CD8 APC-eF780 = 2x10^2, Y = IFNγ FITC (all events)
8: X = CD4 PerCP Cy5.5 = 1x10^3(upper limit), Y = IFNγ FITC (all events)
6a: X = IFNγ FITC = 5x10^2, Y = IL-2 BV650 = 3x10^3
6b: X = IFNγ FITC (all events), Y = TNFα PE-Cy7 = 9x10^2
6c: X = IFNγ FITC (all events), Y = IL-5 PE = 1x10^3
6d: X = IFNγ FITC (all events), Y = IL-13 APC = 1x10^3
6e: X = IFNγ FITC (all events), Y = CD107a PE-Cy7 = 1x10^4

n.b Gate 4 represents the parent gate for both gates 5 and 7.

☒ Tick this box to confirm that a figure exemplifying the gating strategy is provided in the Supplementary Information.